

# Intracellular Hedgehog signaling controls Th17 polarization and pathogenicity

**Joachim Hanna**

CRUK Cambridge Institute <https://orcid.org/0000-0002-2055-1462>

**Louise O'Brien**

CRUK Cambridge Institute

**Chrysa Kapeni**

CRUK Cambridge Institute <https://orcid.org/0000-0003-0408-2106>

**Hung-Chang Chen**

CRUK Cambridge Institute <https://orcid.org/0000-0002-2849-6752>

**Valentina Carbonaro**

CRUK Cambridge Institute <https://orcid.org/0000-0003-0915-6901>

**Alexander Kim**

CRUK Cambridge Institute <https://orcid.org/0000-0002-6425-4566>

**Flavio Beke**

CRUK Cambridge Institute

**Timon E. Adolph**

Medical University Innsbruck

**Mikkel-Ole Skjoedt**

Institute for Immunology and Microbiology, University of Copenhagen <https://orcid.org/0000-0003-1306-6482>

**Karsten Skjoedt**

University of Southern Denmark <https://orcid.org/0000-0002-9161-8185>

**Marc de la Roche**

Dept of Biochemistry, University of Cambridge <https://orcid.org/0000-0002-3757-082X>

**Maïke de la Roche** (✉ [maïke.delaroch@cruk.cam.ac.uk](mailto:maïke.delaroch@cruk.cam.ac.uk))

CRUK Cambridge Institute <https://orcid.org/0000-0002-0558-4119>

---

## Research Article

**Keywords:** Hedgehog signalling, Th17, Gli3, inflammatory bowel disease

**Posted Date:** February 9th, 2021

**DOI:** <https://doi.org/10.21203/rs.3.rs-193347/v1>

**License:**  This work is licensed under a Creative Commons Attribution 4.0 International License.

[Read Full License](#)

---

## Intracellular Hedgehog signaling controls Th17 polarization and pathogenicity

5 Joachim Hanna<sup>1</sup>, Louise O'Brien<sup>1</sup>, Chrysa Kapeni<sup>1</sup>, Hung-Chang Chen<sup>1</sup>, Valentina Carbonaro<sup>1</sup>, Alexander Kim<sup>1</sup>, Flavio Beke<sup>1</sup>, Timon E. Adolph<sup>2</sup>, Mikkel-Ole Skjoedt<sup>3,4</sup>, Karsten Skjoedt<sup>5</sup>, Marc de la Roche<sup>6</sup>, and Maïke de la Roche<sup>1,§</sup>

10 <sup>1</sup> University of Cambridge, Cancer Research UK Cambridge Institute, Robinson Way, Cambridge CB2 0RE, UK

<sup>2</sup> Department of Internal Medicine I, Gastroenterology, Hepatology & Endocrinology, Medical University Innsbruck, Innsbruck, Austria

15 <sup>3</sup> Rigshospitalet - University Hospital Copenhagen, Blegdamsvej 9, 2100 Copenhagen, Denmark

<sup>4</sup> Institute of Immunology and Microbiology, University of Copenhagen, Blegdamsvej 3B, 2200 Copenhagen, Denmark

<sup>5</sup> University of Southern Denmark, J.B.Winslows Vej, 5000 Odense C, Denmark

20 <sup>6</sup> University of Cambridge, Department of Biochemistry, Tennis Court Road, Cambridge CB2 1QW, UK

<sup>§</sup> Corresponding author. Email: [maïke.delaroché@cruk.cam.ac.uk](mailto:maïke.delaroché@cruk.cam.ac.uk) (M.d.I.R.)

25

30

35

## ABSTRACT

40 T helper 17 (Th17) cells play a key role in barrier protection against fungal and bacterial pathogens but are also pathological drivers of many inflammatory diseases. Although the transcription factor networks governing Th17 differentiation are well defined, the signaling pathways that regulate the development and function of this important CD4<sup>+</sup> T cell subset are still poorly understood. Hedgehog (Hh) signaling plays important roles in regulating cell fate decisions during embryogenesis and adult tissue patterning. Using novel CD4-  
45 specific Hh knockout mice, we find that intracellular Hh signaling, independently of exogenous Hh ligands, selectively drives Th17 lineage differentiation but not the development of Th1, Th2, or iTreg CD4<sup>+</sup> Th cells. We show that the endogenous Indian Hh (Ihh) ligand signals via the signal transducer Smoothened to activate both canonical and non-canonical Hh pathways, through the Gli3 transcription factor and AMPK  
50 phosphorylation, respectively. Using two models of intestinal inflammation, we demonstrate that inhibition of the Hh pathway with either the clinically approved small molecule inhibitor vismodegib or genetic ablation of Ihh in CD4<sup>+</sup> T cells greatly diminishes disease severity. Taken together, we have uncovered Hh as a novel signaling pathway controlling Th17 differentiation and Gli3 as a crucial transcription factor in this process.  
55 Our work paves the way for a potential use of Hh inhibitors in the treatment of inflammatory bowel disease and other autoimmune diseases.

## INTRODUCTION

60 The adaptive immune system is able to initiate highly tailored immune responses. After antigenic stimulation, naïve CD4<sup>+</sup> T cells can differentiate into specialized T helper (Th) cell lineages (Th1, Th2, Th17 and Tregs), characterized by the production of key effector cytokines that dominate subsequent immune responses. Th lineages are each able to  
65 respond to different classes of immune challenges. Th1 cells secrete IFN $\gamma$  to promote immunity against intracellular pathogens, while Th2 cells secrete IL-4, IL-5 and IL-13 to respond to parasitic and helminth infection. Th17 cells produce IL-17 and IL-22 required

for clearance of extracellular pathogens, while Tregs suppress immune responses (reviewed in <sup>1</sup>).

70

This lineage-specific fate decision is hence of great importance and is governed by environmental signals received by the CD4<sup>+</sup> T cell. These include the mechanism through which the T cell is activated by antigen presenting cells (APCs) and the strength of T cell receptor (TCR) signaling. Perhaps most critical are signals from the extracellular cytokine milieu which initiate intracellular STAT and SMAD signaling. These factors drive the induction of lineage-specific and lineage-associated transcription factors to promote and reinforce Th lineage fate choice <sup>2</sup>.

75

Th17 differentiation is initiated by TGF $\beta$  and inflammatory cytokines, which signal through SMAD2 and STAT3, respectively, to induce the Th17 differentiation program; this is guided by a number of transcription factors including the 'master' transcription factor ROR $\gamma$ t <sup>3</sup>. However, although the transcription factor network governing Th17 identity has been well described <sup>4</sup>, the intracellular signaling pathways regulating this complex differentiation program are less clear.

85

Th17 cells are critical for maintaining the integrity of intestinal barrier surfaces and coordinating the immune response against pathogenic extracellular bacteria and fungi. However, Th17 cells are also key drivers of autoimmune diseases including inflammatory bowel disease (IBD), rheumatoid arthritis and multiple sclerosis <sup>5</sup>. There is therefore strong clinical interest to specifically inhibit differentiation and pathogenicity of these cells.

90

The Hedgehog (Hh) pathway has key functions in regulating cell fate choices throughout metazoan development and adult tissue homeostasis by regulating tissue patterning, cell proliferation and differentiation <sup>6</sup>. Vertebrate Hh signaling critically depends on the primary cilium, where the pathway is initiated upon binding of extracellular Sonic, Desert or Indian Hh ligands (Shh, Dhh, Ihh) to the transmembrane receptor Patched (Ptch) on a Hh-responsive cell. Ligand binding to Ptch allows the transmembrane protein Smoothed (Smo) to translocate into the primary cilium, where it activates the glioma-associated

95

100 oncogene (Gli) family of transcription factors (Gli1, 2, or 3). These translocate to the nucleus and initiate the transcription of Hh target genes<sup>6,7</sup>.

In the immune system, the Hh signaling pathway has been implicated in T cell development in the thymus<sup>8</sup>. Given the structural and morphological similarities between  
105 the primary cilium and immune synapses<sup>9,10</sup>, we were prompted to study Hh signaling in mature T cells<sup>11</sup>. TCR signaling at the immune synapse upregulates Hh components in CD8<sup>+</sup> T cells independently of exogenous Hh ligands, which we have shown to be important for CD8<sup>+</sup> T cell killing. Our data raised the possibility that Hh signaling in CD8<sup>+</sup> T cells may occur intracellularly<sup>11</sup>. By contrast, less is known about Hh signaling in mature  
110 CD4<sup>+</sup> T cells. One study has shown that transgenic expression of Gli2 activator and repressor forms in CD4<sup>+</sup> T cells can influence Th2 differentiation<sup>12</sup>, but the role of endogenous Hh signaling in Th polarization is not known.

Here, we find that Hh signaling is functionally important for Th17 differentiation but not Th1, Th2, and iTreg CD4<sup>+</sup> T cell development. While conventional Hh signaling involves  
115 paracrine signaling – in which Hh ligand is secreted from one cell and signals to another cell that expresses the Hh receptor – we discovered that in CD4<sup>+</sup> T cells Hh signaling is intracellular and is mediated by Ihh, Smo and Gli3. Mechanistically, Smo activates Gli3 which is needed for the induction of IL-17a, and also regulates metabolic fitness in Th17 cells in a non-canonical fashion through AMPK phosphorylation. Functionally, we show  
120 that blocking Hh signaling *in vivo* genetically or with small molecule Hh inhibitors ameliorates disease in two models of Th17-driven inflammatory bowel disease.

## RESULTS

### 125 **Core Hedgehog (Hh) signaling components are specifically upregulated in Th17** 130 **cells**

Previous work has suggested that Hh components Smo and Ptch are expressed in CD4<sup>+</sup> T cells <sup>13</sup>. We extended these analyses by comprehensively profiling Hh ligands, receptors, signal transducer and transcription factors (Fig. 1A) throughout CD4 Th differentiation in an established *in vitro* polarization protocol (Suppl. Fig. 1) by western blot, immunofluorescence and quantitative RT-PCR.

The Hh ligand Dhh was not detected in any of the Th lineages and only the Th2 subset expressed and upregulated *Shh* mRNA post day 3 (Suppl. Fig. 2). By contrast, *Ihh* was the only Hh ligand already present in naïve CD4<sup>+</sup> T cells and was expressed throughout 135 Th17 differentiation (Fig. 1B). Hh receptors Ptch1 and Ptch2 were expressed in all lineages with Ptch1 being predominantly expressed (Suppl. Fig. 2, Fig. 1C). Smo mRNA was also detected in all Th lineages but showed most pronounced upregulation in Th17 cells on day 3 of culture (Suppl. Fig. 2). Since Smo is the key signal transducer of the Hh pathway, we wanted to follow up on this observation with the analysis of Smo protein. As 140 no functional anti-Smo antibodies were commercially available, we generated novel monoclonal antibodies directed against the C-terminus of Smo (Suppl. Fig. 3) and show that only the Th17 lineage expresses strikingly high levels of Smo protein on day 3 and day 5 (Fig. 1C). Using our new monoclonal antibody, we find that Smo resides on the plasma membrane and on intracellular vesicles as has been described for CD8<sup>+</sup> T cells 145 previously <sup>11</sup> (Fig. 1D).

Vertebrate Hh signaling activity can be evaluated by the expression of the downstream Gli transcription factors <sup>14</sup>. All lineages apart from Th2 modestly upregulated *Gli1* upon Th polarization. Given its potential to regulate Th2 differentiation <sup>12</sup>, we were interested in assessing *Gli2* expression. However, we were unable to detect *Gli2* transcripts in any 150 of the conditions tested (Suppl. Fig. 2). Strikingly, *Gli3* was the only transcription factor showing lineage-specific expression in Th17 and iTreg T cells peaking at day 3 of culture (Fig. 1E).

155 Taken together, while all lineages expressed core Hh components, only Th17 cells express high levels of Smo, as well as Gli1 and Gli3 transcription factors by day 3 of culture when lineage choice is specified. Furthermore, Ihh is the only Hh ligand expressed in Th17 cells.

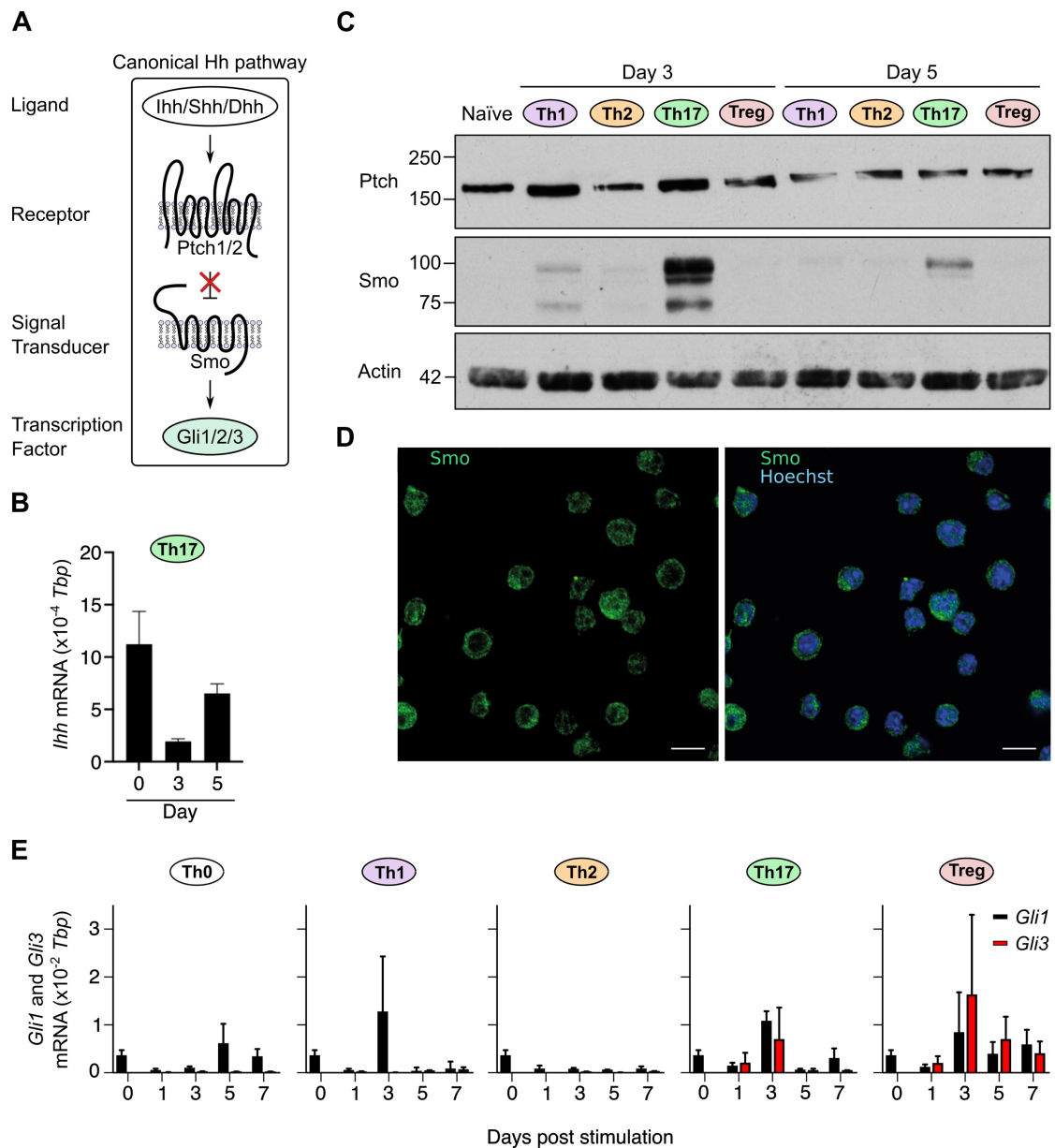


**Figure 1: Key Hedgehog signaling components are induced in Th17 cells.** (A) Overview of canonical Hh signaling. (B-E) Naïve CD4<sup>+</sup> T cells were purified from spleen and peripheral lymph nodes of C57BL/6 mice and stimulated with plate-bound anti-CD3 $\epsilon$ /CD28 antibodies in the presence of polarizing cytokines to generate Th0, Th1, Th2, Th17 and Treg subsets. (B) Expression of *Ihh* was assessed by qRT-PCR in naïve CD4<sup>+</sup> T cells and Th17 cells at the indicated timepoints after TCR stimulation. Data is normalized to *Tbp* as a reference gene. n = 3 independent experiments. (C) Immunoblot analysis of Ptch and Smo in naïve CD4<sup>+</sup> T cells and T helper (Th) subsets at indicated timepoints post stimulation. n = 2 (naïve) or 3 (Th subsets) independent experiments. (D) Immunofluorescence imaging (single x-y confocal section) of Th17 cells at day 3 labelled with antibodies against Smo (green). Nuclei were stained with Hoechst (blue). Scale bars: 10 $\mu$ m. (E) Expression of *Gli1*, *Gli2* and *Gli3* were assessed by qRT-PCR in Th subsets at indicated timepoints post stimulation in the presence of polarizing cytokines. Data is normalized to *Tbp* as a reference gene with similar results obtained when using CD3 $\epsilon$  as a reference gene. n = 3 independent experiments. *Gli2* mRNA was undetectable in all conditions tested.

**Th17 lineage-polarizing cytokines induce the expression of central Hh signaling components.**

175

Th17 lineage polarization is initiated when naïve CD4<sup>+</sup> T cells recognize cognate antigen on APCs in the presence of a cytokine milieu dominated by IL-6, TGFβ, IL-1β and IL-23. Given the Th17-specific upregulation of Smo and *Gli1/Gli3* (Fig.1), we asked whether Th17-inducing cytokines play a role in the induction of these Hh signaling components.

180

First, we titrated TGFβ in the presence of fixed concentrations of IL-6, IL-23, and IL-1β and assessed *Gli1* and *Gli3* levels by qRT-PCR and Smo by western blot. Strikingly, *Gli3* but not *Gli1* expression was upregulated by TGFβ in a dose-dependent manner (Fig. 2A, upper panel), which is critically dependent on the presence of IL-6. 1 μM TGFβ led to optimal IL-17a expression (Suppl. Fig 4) and highest Smo levels (Fig. 2A, lower panel).

185

Interestingly, IL-6 alone was necessary and sufficient to induce Smo protein and stepwise addition of TGFβ, IL-23, and IL-1β increased not only IL-17a production (Suppl. Fig 4A) but also *Gli3* RNA expression levels (Fig. 2B, upper panel) as well as Smo protein (Fig. 2B, lower panel). Thus, two distinct Th17 lineage polarizing cytokines, TGFβ and IL-6, promote the expression of central Hh components *Gli3* and Smo, respectively.

190

**Exogenous Indian Hedgehog (Ihh) does not affect Th17 polarization.**

In the canonical pathway, Hh signaling is initiated upon binding of the exogenous Hh ligand, generated by Hh-producing cells, to the receptor Ptch on the plasma membrane of Hh-responsive cells <sup>7</sup>. We wondered whether exogenous Hh ligand could promote

195

Th17 polarization under Th0 stimulation conditions or in the presence of low (IL-6 alone), intermediate (IL-6 and TGFβ), or strong (IL-6, TGFβ, IL-23, and IL-1β) Th17 polarizing conditions (Fig. 2C, Suppl. Fig 4B). Surprisingly, even high concentrations of active Ihh N-peptide were unable to promote Th17 differentiation in any condition tested. This points towards a novel intracellular form of Hh signaling in CD4<sup>+</sup> T cells.

200

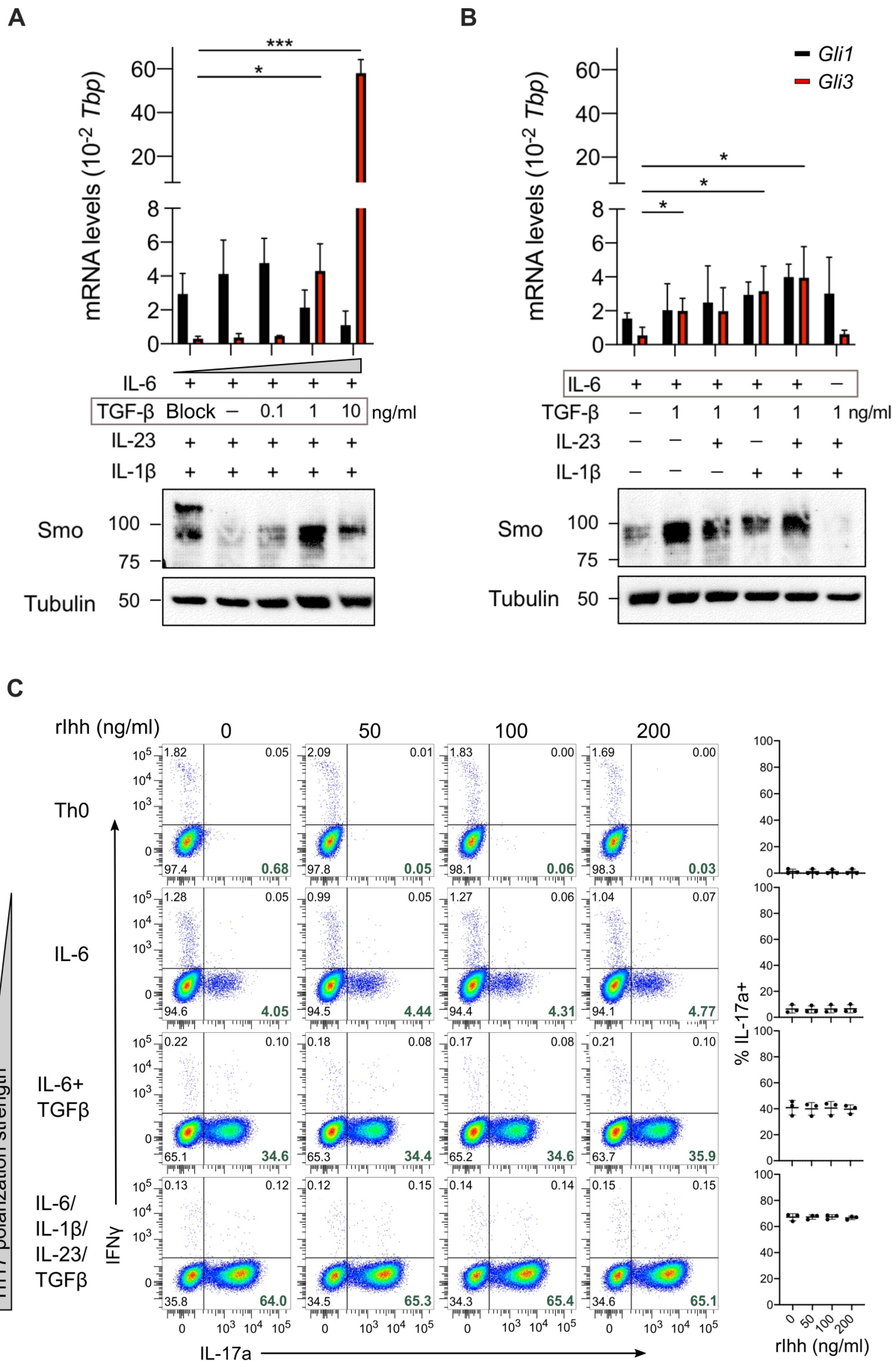


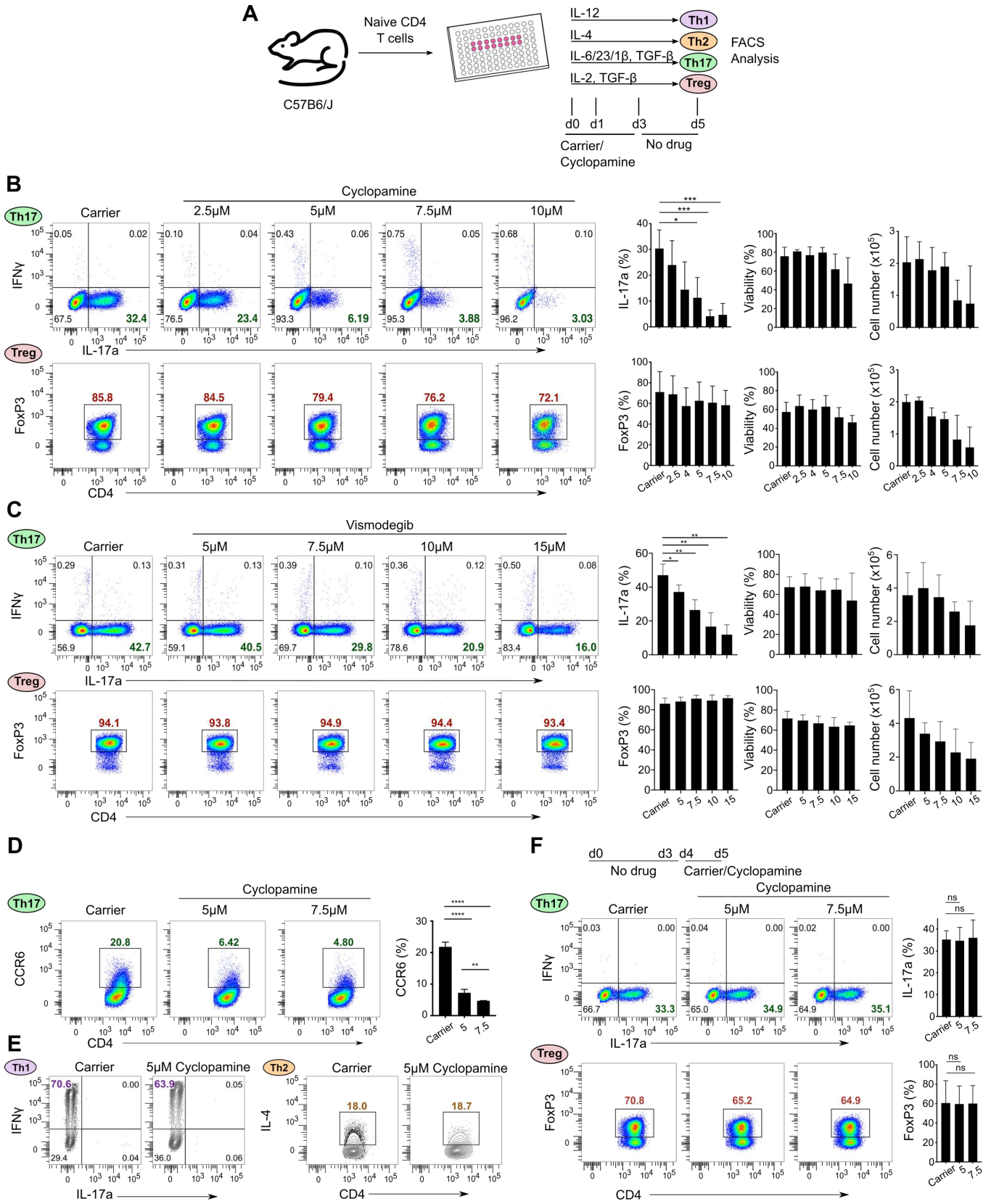
Figure 2

205 **Figure 2: IL-6 and TGF $\beta$  but not exogenous lhh ligand are the primary inducers of Hh signaling in Th17 cells.** (A-C) Naïve CD4<sup>+</sup> T cells were purified from spleen and peripheral lymph nodes of C57BL/6 mice and polarized with the indicated polarizing cytokines. (A, B) Cells were harvested at day 3 post stimulation for immunoblot analysis of Smo and qRT-PCR analysis of *Gli1* and *Gli3*. TGF $\beta$  blocking antibody (clone: 1D11) was added in the indicated condition for the duration of polarization at 10 $\mu$ g/ml. Data is normalized to *Tbp* as a reference gene. Similar results were obtained when *CD3 $\epsilon$*  was used as a reference gene. n = 3 independent experiments. (C) Naïve CD4<sup>+</sup> T cells were stimulated with the indicated polarizing cytokines in the presence or absence of recombinant N-terminal murine lhh fragment at the indicated concentrations. All cells were polarized in the presence of anti-IFN $\gamma$  and anti-IL4 blocking antibodies and were harvested for analysis by FACS on day 5. Representative flow cytometry plots of n = 3 independent experiments are shown with a summary on the right. Data are means +/- SD. p-values were calculated using an unpaired two-tailed Student's t test. \* p<0.05, \*\* p<0.01, \*\*\* p<0.001.

### **Small molecule Hedgehog inhibitors selectively impair Th17 polarization *in vitro*.**

220 Hh signaling can be efficiently blocked by small molecule inhibitors of the key signal transducer Smo. We investigated the effect of Hh inhibitor cyclopamine on CD4<sup>+</sup> Th lineage polarization by treating T cell cultures with inhibitor for the first 3 days (when lineage identity is determined *in vitro*) and assessing lineage identity on day 5 (Fig. 3A). Strikingly, only Th17 (IL-17a, top row) but not Treg (FoxP3, bottom row) polarization was compromised in a dose-dependent manner (Fig. 3B). Viability and cell number of Th17 cells were not significantly affected at the inhibitor concentrations used (Fig. 3B, last two columns). Similar results were obtained with clinically approved Smo inhibitor vismodegib<sup>15</sup> (Fig. 3C). Cyclopamine treatment also downregulated surface CCR6 expression, a hallmark protein of Th17 cells, in a dose-dependent manner (Fig. 3D) but did not affect Th1/Th2 differentiation (Fig. 3E). The same dose-dependent downregulation of CCR6 was also seen in vismodegib-treated Th17 cells (Suppl. Fig 5).

230 Next, we investigated the window of active Hh signaling during *in vitro* CD4<sup>+</sup> T cell differentiation. For this, we limited the Hh inhibitor treatment to the last 24h of the 5-day Th17 and Treg differentiation culture before assaying them by flow cytometry on day 5 (Fig. 3F). Interestingly, we found that inhibition of Hh signaling post day 4 did not affect IL-17a production or FoxP3 levels indicating that Hh signaling is active in the first 3 days of culture. These results fit nicely with the high expression of Hh signaling components during this time. Taken together, we found that Hh signaling is crucial for Th17 polarization but not Th1, Th2, or iTreg differentiation.



240

Figure 3

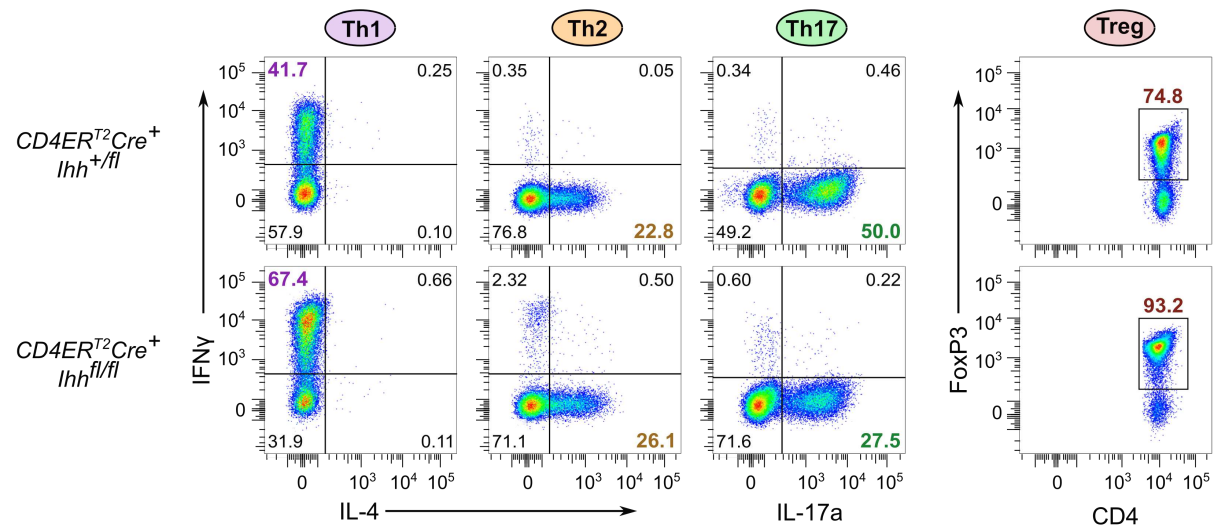
**Figure 3: Small molecule Hh inhibitors selectively block Th17 polarization *in vitro*.** (A) Schematic overview of Hh inhibitor cyclopamine administration schedule. (B) Naïve CD4<sup>+</sup> T cells were stimulated under Th17 or Treg polarizing conditions in the presence of the indicated doses of cyclopamine or carrier control for three days. Cells were harvested for analysis by flow cytometry on day 5. Quantitation of IL-17a/FoxP3 expression, viability measured by absence of live/dead staining, and cell numbers are shown on the right. n = 4 independent experiments. (C) Naïve CD4<sup>+</sup> T cells were stimulated under Th17 or Treg polarizing conditions in the presence of the indicated doses of vismodegib or carrier control for five days. Cells were harvested for analysis by flow cytometry on day 5. Quantitation of IL-17a/FoxP3 expression, viability measured by absence of live/dead staining, and cell numbers are shown on the right. n = 3 independent experiments. (D) Naïve CD4<sup>+</sup> T cells were stimulated under Th17 polarizing conditions in the presence of the indicated doses of cyclopamine or carrier control for three days. Cells were harvested for analysis by flow cytometry on day 5. Quantitation of cell-surface CCR6 is shown on the right. n = 3 independent experiments. (E) Naïve CD4<sup>+</sup> T cells were stimulated under Th1 or Th2 polarizing conditions in the presence of 5µM cyclopamine or carrier control for three days. Cells were harvested for analysis by flow cytometry on day 5. n = 3 independent experiments. (F) Naïve CD4<sup>+</sup> T cells were stimulated under Th17 or Treg polarizing conditions in the presence of the indicated dose of cyclopamine or carrier control for the final 24h of polarization. Cells were harvested for analysis by flow cytometry on day 5. n = 3 independent experiments. Data are means +/- SD. p-values were calculated using an unpaired two-tailed Student's t test. \* p<0.05, \*\* p<0.01, \*\*\* p<0.001.

### 265 **Conditional ablation of Hh components in CD4<sup>+</sup> T cells impairs Th17 polarization *in vitro*.**

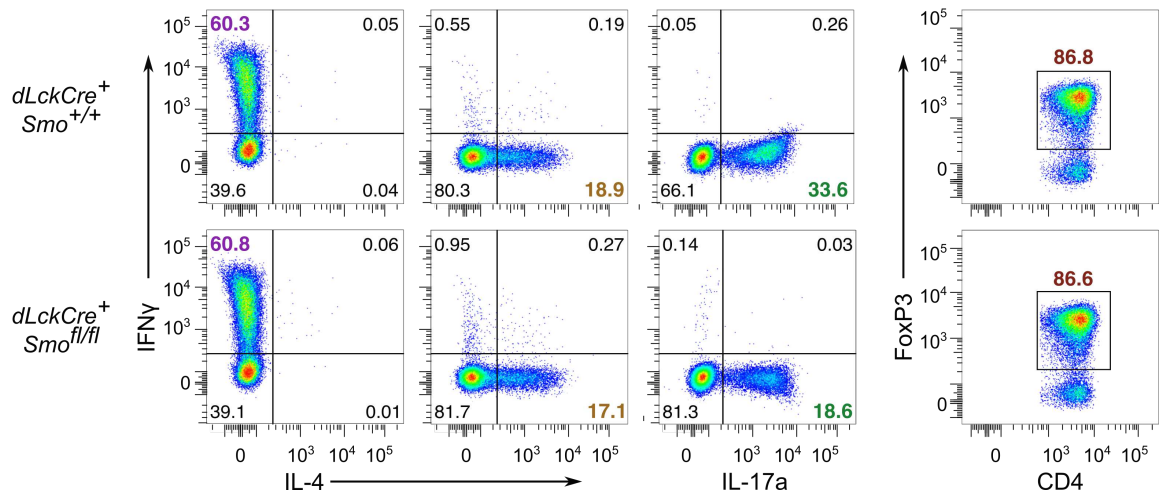
To confirm our results genetically, we generated two independent conditional Hh knockout models: one using the *CD4ERT2Cre* where the Hh ligand Indian Hh (*Ihh*) can be inducibly deleted in naïve CD4<sup>+</sup> T cells upon administration of tamoxifen and the other making use of the *dLckCre* which leads to ablation of *Smo* after completion of T cell development in the thymus. The *CD4ERT2Cre Ihh<sup>fllox</sup>* model is very important to prove that Hh signaling is truly intracellular in CD4<sup>+</sup> T cells and not dependent on exogenous ligands. Knockout mice from both models had phenotypically normal peripheral T cell compartments (Suppl. Fig. 6A,B,D). Importantly, we were able to conclusively validate the data obtained from the inhibitor studies: loss of *Ihh* (Fig. 4A) or *Smo* in CD4<sup>+</sup> T cells (Fig. 4B) resulted in diminished Th17 lineage polarization compared with control cells while Th1, Th2, and Treg differentiation remained unaffected.

Thus, we firmly established a selective requirement for Hh signaling in Th17 polarization but not Th1, Th2, and Treg differentiation.

A



B



280

**Figure 4: Conditional knockout of Hh signaling components *Ihh* and *Smo* in CD4<sup>+</sup> T cells leads to diminished Th17 polarization but does not affect other Th lineages.** Naïve CD4<sup>+</sup> T cells were purified from spleen and peripheral lymph nodes of either *CD4ER<sup>T2</sup>Cre<sup>+</sup> Ihh<sup>+/fl</sup>* (HET) and *Ihh<sup>fl/fl</sup>* (KO) C57BL/6 mice (A), or *dLckCre<sup>+</sup> Smo<sup>+/+</sup>* (WT) and *dLckCre<sup>+</sup> Smo<sup>fl/fl</sup>* (KO) C57BL/6 mice (B). (A,B) Cells were stimulated under Th1, Th2, Th17 or Treg polarizing conditions and harvested for analysis by flow cytometry on day 5. n=2-3 mice per genotype.

285

290 **Hh signaling controls Th17 polarization *in vivo*.**

Th17 cells are critical drivers of inflammatory bowel disease including pathological inflammation of the small intestine. A model of small intestinal inflammation driven by Th17 cells was developed by the Flavell lab<sup>16</sup>. Here, the intraperitoneal injection of anti-CD3 antibodies leads to polarization and accumulation of Th17 cells in the small intestine within 3 days. Using this model system we treated wildtype C57BL/6 mice by oral gavage

295

with either carrier or Hh inhibitor vismodegib, which has been clinically approved for oral use (Fig. 5A). Strikingly, intestinal inflammation was ameliorated in vismodegib-treated mice. Mice, in which Hh signaling had been inhibited, showed reduced weight loss (Fig. 5B) and less thickening and shortening (lower Weight/Length ratio) of the small intestine (Fig. 5C). Importantly, vismodegib-treated mice had significantly fewer Th17 intraepithelial lymphocytes (IELs) while the number of IFN $\gamma$ <sup>+</sup> IL17<sup>neg</sup> IELs was less affected (Fig. 5D). This was accompanied by a 50% reduction of IL-17a levels in the serum (Fig. 5E).

In order to prove genetically that Hh signaling is instrumental to induce Th17-mediated colitis we used cells from our novel inducible *Ihh* KO mice in a T cell adoptive transfer colitis model<sup>17</sup>. For this, we treated *CD4ER<sup>T2</sup>CreIhh<sup>fl/fl</sup>tdTom* (KO) and *CD4ER<sup>T2</sup>CreIhh<sup>fl/+</sup>tdTom* (HET) mice with tamoxifen to induce the deletion of *Ihh* in CD4<sup>+</sup> T cells. Next, we flow sorted naïve, tdTom<sup>+</sup> CD45RB<sup>hi</sup> CD25<sup>-</sup> CD4<sup>+</sup> T cells from HET and KO mice, adoptively transferred them into T-cell deficient *Rag2<sup>-/-</sup>* recipient mice and assessed inflammatory disease activity (Fig. 5F).

While transfer of *Ihh* HET CD4<sup>+</sup> T cells potently induced colitis, transfer of *Ihh* KO CD4<sup>+</sup> T cells showed strongly diminished colitis indicated by reduced weight loss (Fig. 5G), reduced colon thickening/shortening (Fig. 5H) and reduced mucosal infiltration of T cells expressing IL-17a, IL-22 and IFN $\gamma$  in the colon (Fig. 5I). In line with this, histological analysis revealed that *Ihh* HET CD4<sup>+</sup> T cells potently induced colitis in *Rag2<sup>-/-</sup>* recipient mice which was characterized by mononuclear and polymorpho-nuclear mucosal to submucosal infiltration of inflammatory cells, crypt hyperplasia and epithelial injury. In contrast, transferred *Ihh* KO CD4<sup>+</sup> T cells were strongly impaired in their ability to induce colitis and mice showed minimal signs of inflammatory disease in the colon (Fig. 5J). No effect was observed in mesenteric lymph nodes and spleens (Suppl. Fig. 9).

Taken together, we demonstrate for the first time that intracellular Hh signaling is a critical driver of Th17 polarization in chronic intestinal inflammation models of human inflammatory bowel disease (IBD). Importantly, we show that the small molecule Hh inhibitor vismodegib, which is clinically approved by the EMA/FDA, effectively protected against IBD.

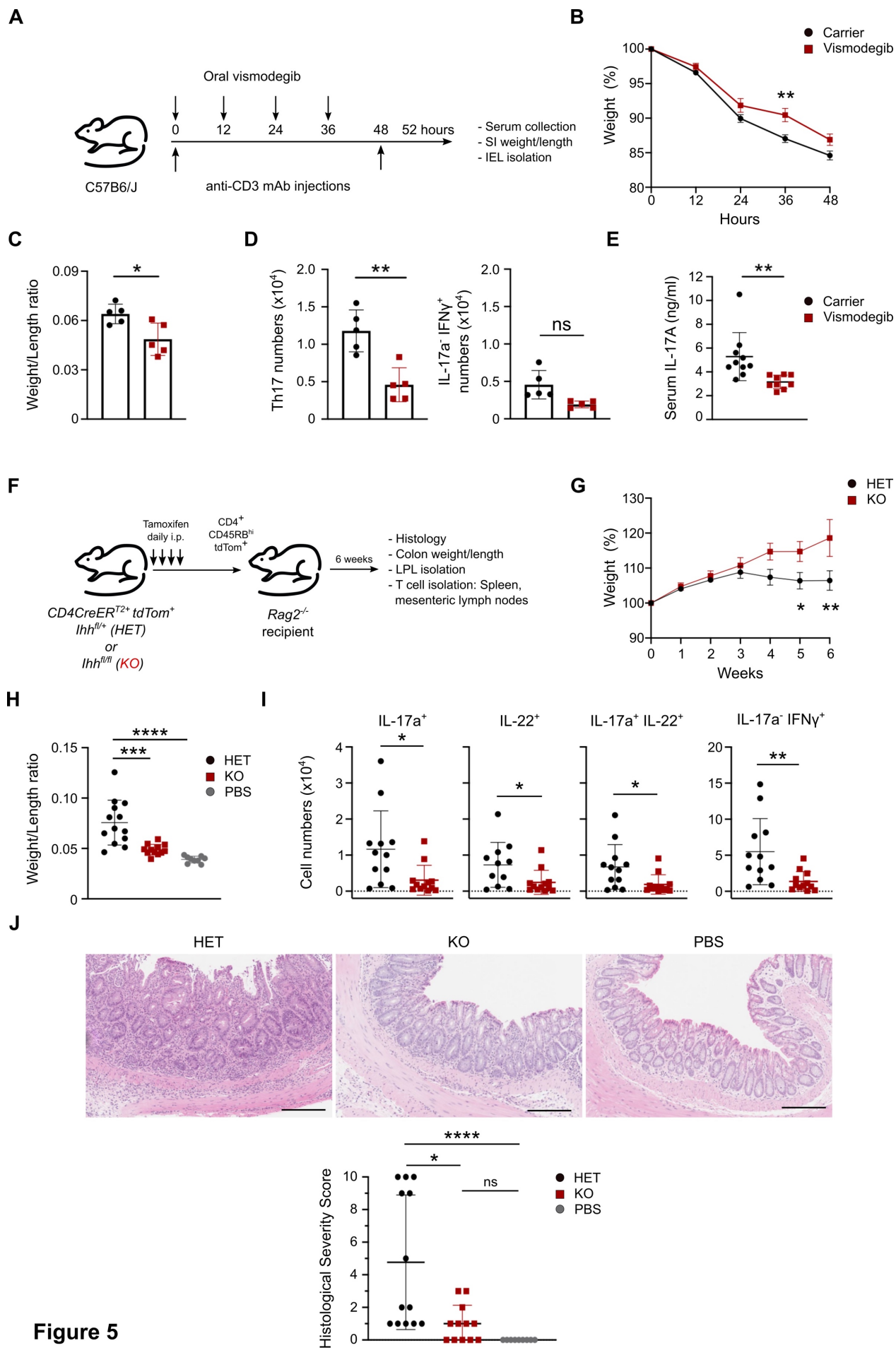


Figure 5

**Figure 5: Hh signaling is critical for Th17 responses *in vivo*.** (A) C57BL/6 mice were injected *i.p.* with 20  $\mu$ g anti-CD3 monoclonal antibody (Clone: 145-2C11) at 0h and 48h and dosed every 12h by oral gavage with 100 mg/kg vismodegib or carrier control. Mice were harvested at 52h. (B) Weight loss during the course of the experiment. Pooled data from three independent experiments. (C) Small Intestine weight/length ratios. Representative data shown from one of three independent experiments. (D) IEL Th17 and IFN $\gamma$ <sup>+</sup> IL-17a<sup>-</sup> CD4<sup>+</sup> T cell numbers. Representative data shown from one of three independent experiments. Gating strategy is shown in Suppl. Fig. 7. (E) Serum IL-17a concentrations at 52h. Pooled data from three independent experiments. p-values were calculated using an unpaired two-tailed Student's t test. \* p<0.05, \*\* p<0.01. (F) *Rag2*<sup>-/-</sup> mice were injected *i.p.* with 4x10<sup>5</sup> CD45RB<sup>hi</sup> CD25<sup>neg</sup> tdTom<sup>+</sup> CD4<sup>+</sup> T cells isolated from the spleens and peripheral lymph nodes of *CD4<sup>ERT2</sup>Cre Ihh<sup>fl/+</sup>* (HET) or *CD4<sup>ERT2</sup>Cre Ihh<sup>fl/fl</sup>* (KO) mice. Mice were harvested at 6-7 weeks. (G-J) pooled data from three independent experiments shown. (G) Weight loss during the course of the experiment. (H) Colon weight/length ratios. (I) Numbers of IL-17a<sup>+</sup>, IL-22<sup>+</sup>, IL-17a<sup>+</sup> IL-22<sup>+</sup>, IFN $\gamma$ <sup>+</sup> IL-17a<sup>neg</sup> T cells isolated from colonic lamina propria. Gating strategy is shown in Suppl. Fig. 8. (J) Panels on the top show representative H&E staining of the recipient mouse colons. Panel on the bottom shows quantification of histological severity scored blindly by a gastroenterologist. Scale bars: 200 $\mu$ m. Data are means  $\pm$  SEM (B,G). Rest are means  $\pm$  SD. p-values were calculated using an unpaired two-tailed Student's t test. \* p<0.05, \*\* p<0.01, \*\*\* p<0.001. (J) p-values were calculated using an unpaired two-tailed Student's t test (C,D,E,I), a Kruskal-Wallis test (J), a one-way ANOVA (H) or a two-way ANOVA with Sidak correction (B,G). \* p<0.05, \*\* p<0.01, \*\*\* p<0.001.

350

### **Proximal cytokine signaling and levels of master Th17 transcription factors are not affected by loss of Hh signaling.**

Having established that Hh signaling is functionally important for Th17 polarization, we sought to determine the mechanism for this effect. Downstream of the IL-6 and IL-23 cytokine receptors, Th17 differentiation is initiated by STAT3 phosphorylation which in turn translocates to the nucleus and initiates the transcription of key Th17 polarizing transcription factors (TFs). We found that phosphoSTAT3 (pSTAT3) levels are unaltered upon IL-6 stimulation when we inhibit the Hh pathway with cyclopamine in Th17 cells, indicating that Th17-initiating cytokine signaling is not altered by the Hh pathway (Fig. 6A).

Next, we profiled the expression of master Th17 TFs<sup>18</sup> in Th17 cells treated with Hh inhibitor cyclopamine or carrier control (Fig. 6B). Although *Il17a* mRNA was markedly reduced in our treatment conditions, the Th17-regulating TFs *Rorct*, *Rora*, *Irf4*, *Runx1*, and *Batf* were not majorly affected and neither was a novel Th17-associated TF *Vax2*<sup>19</sup>. To interrogate the mechanism of Hh-mediated Th17 polarization more globally we performed RNA-Seq analysis of Th17 cells polarized in the presence of carrier control or

365

Hh inhibitor cyclopamine. As expected, expression of known Hh target genes<sup>20</sup> like *Smo*, *Jag2*, *Prdm1*, and *Fst* was significantly reduced in Hh inhibitor-treated cells (Fig. 6C). The expression level of master Th17 TFs in Hh inhibitor-treated Th17 cells was ambiguous: while for example *Rora* and *Batf* were significantly reduced upon inhibitor treatment, *Junb* and *Runx1* were increased (Fig. 6C). Th17 cells have stem-cell like features: plasticity and self-renewal<sup>21</sup>. Interestingly, we find that *Tcf7*, the key stem cell-associated gene in Th17 cells<sup>22</sup>, as well as other Wnt target genes were downregulated in Hh inhibitor-treated cells (Fig. 6C) suggesting that Hh signaling may be critical to endow Th17 cells with stem cell properties.

Overall, GSEA (Gene Set Enrichment Analysis) certified that Hh inhibitor-treated cells moved away from a Th17 transcriptional profile (Fig. 6D, Suppl. Fig. 10A). However, we show that this effect of Hh signaling blockade is not due to any effects on proximal cytokine signaling or expression levels of key Th17 TFs.

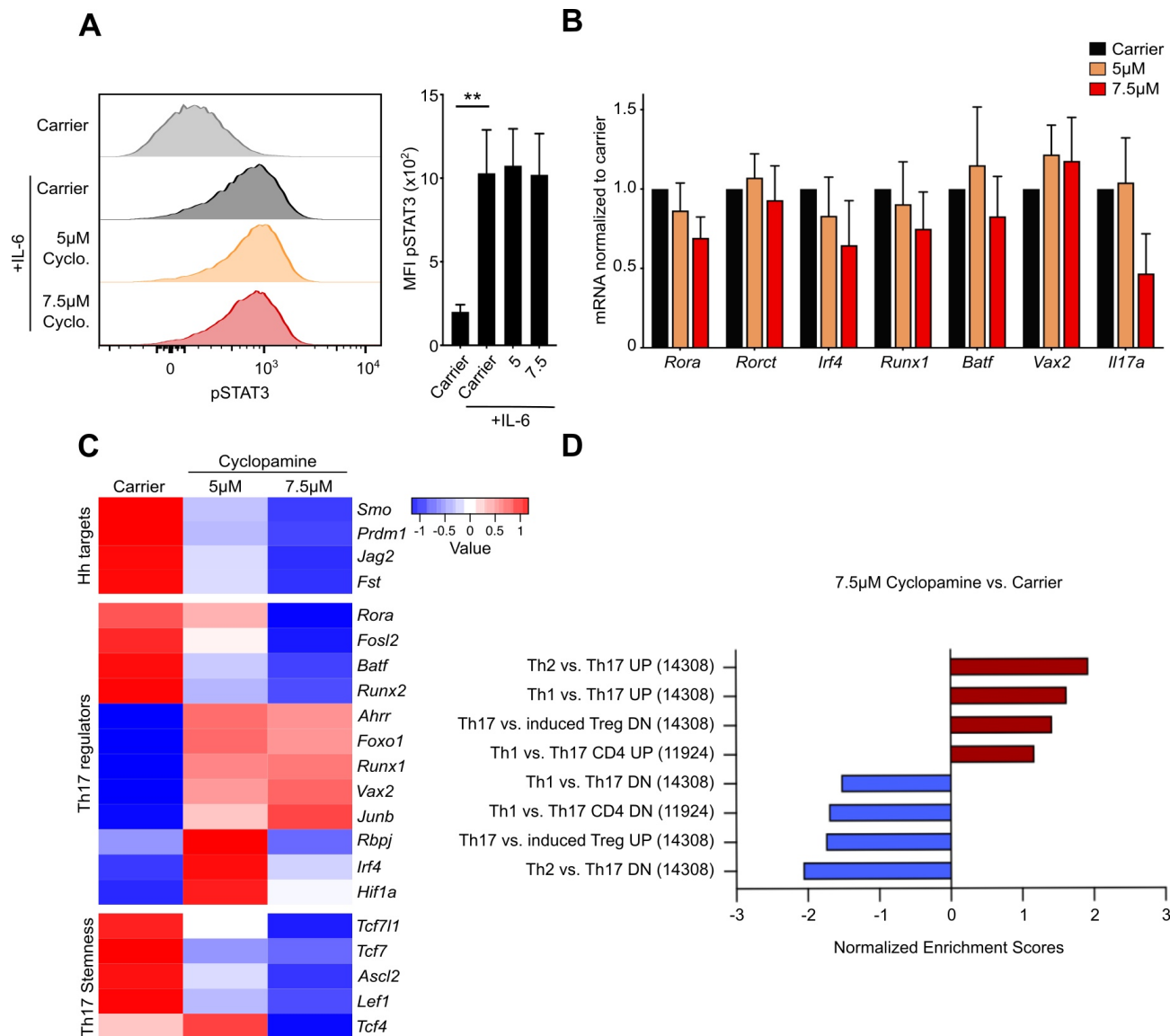


**Figure 6: Mechanistic analysis of Th17-related signaling nodes.** Naïve CD4<sup>+</sup> T cells were purified from spleen and peripheral lymph nodes of C57BL/6 mice and stimulated under Th17 polarizing conditions in the presence of the indicated doses of cyclopamine or carrier control for three days. (A) On day 5, cells were treated with 100ng/ml IL-6 for 15min and harvested for analysis of pSTAT3 levels by flow cytometry. Quantitation of pSTAT3 staining is shown on the right. n = 3 independent experiments. (B) Cells were harvested for analysis at day 3. Expression of *RORA*, *RORct*, *IRF4*, *Runx1*, *BATF*, *Vax2* and *Il17a* were analyzed by qRT-PCR. Data is normalized to *Tbp* as a reference gene. Similar results were obtained when *CD3ε* was used as a reference gene. n = 3 independent experiments. (C) RNASeq analysis of Hh target genes, Th17 regulators and stemness genes. Th17 cells were polarized as described above stimulated in the presence of the indicated doses of cyclopamine or carrier control for three days and harvested at day 3. Six samples/group. (D) Normalized Enrichment Scores (NES) from GSEA of (C) demonstrating a loss of Th17 identity upon Hh inhibitor treatment. Data are means  $\pm$  SD. p-values were calculated using an unpaired two-tailed Student's t test. \*\* indicates  $p < 0.01$ .

**Gli3 is a novel Th17-promoting transcription factor that acts in concert with non-canonical Hh signaling via pAMPK in Th17 polarization.**

400 Smo is the key signal transducer of the Hh pathway and can function in both a canonical and non-canonical fashion (Fig. 7A). Smo activates Gli transcription factors as part of the canonical pathway, but has also been shown to activate AMPK<sup>23</sup> or act through its GTPase activity when associated with non-canonical Hh signaling<sup>24</sup>.

Three transcription factors are associated with Hh signaling, but only Gli1 and Gli3 are expressed in CD4<sup>+</sup> T cells (Fig. 1E, Suppl. Fig. 2). To dissect their relevance, we first investigated the role of Gli1 in CD4<sup>+</sup> T cell polarization. We isolated naïve CD4<sup>+</sup> T cells from *Gli1* knockout mice as well as heterozygous and wildtype littermates (validation, Suppl. Fig. 6C, Fig. 7B left panel) and polarized the cells into Th0, Th1, Th2, Th17, and iTreg cells. Surprisingly, no differences in Th polarization were observed between *Gli1* WT, HET, and KO mice showing that Gli1 is functionally not important for Th17 differentiation (Fig. 7B right panel).

410 Thus, we asked whether Gli3 downstream of canonical Hh signaling was important for Th17 polarization. We polarized Th17 cells from conditional *Ihh* KO or HET control mice as well as Hh inhibitor or carrier control treated Th17 cells and assessed expression levels of *Gli1* and *Gli3* mRNA. While *Ihh* KO and inhibitor treated Th17 cells showed no difference in *Gli1* levels compared to their controls, *Gli3* mRNA was 76% and 52% reduced, respectively (Fig. 7C). Although *Gli1* mRNA is a reporter of active Hh signaling in many other tissues<sup>14</sup>, we show here that in Th17 cells this is not the case and *Gli3* transcript levels instead serve as a faithful reporter of active Hh signaling.

420 A pioneering bioinformatic analysis by Miraldi *et al* using ATACSeq datasets of Th17 cells to analyze Th17 transcriptional regulatory networks identified the top 30 “core” Th17 TFs<sup>19</sup>. Among these “core” TFs were the well-established Th17-inducing TFs Ror $\gamma$ t, Ror $\alpha$ , STAT3, Maf, and Hif1 $\alpha$ . Strikingly, the authors identified Gli3 among these top 30 “core” Th17 TFs and predicted putative gene targets of Gli3. We went back to our RNASeq analysis of Hh inhibitor-treated Th17 cells and assessed the expression of the predicted Gli3 targets. Gli3 can act in two opposing functions at target gene promoters: as a transcriptional repressor when truncated (GliR) or as a transcriptional activator (GliA)<sup>25</sup>.

The balance between GliR and GliA in the nucleus shapes the Hh response. We found that upon Hh inhibitor treatment the majority of the predicted Gli3 target genes increase or decrease in a dose-dependent manner (Fig. 7D, Suppl. Fig. 10B) indicating that indeed Hh-induced Gli3 regulates the transcription of these target genes to control Th17 polarisation.

In order to interrogate the functional relevance of Gli3 we used CRISPR to delete *Gli3* in primary CD4<sup>+</sup> T cells and achieved a 52% reduction of Gli3 RNA by day 3 (Fig. 7E). Importantly, knockout of *Gli3* in a proportion of primary Th17 cells led to a significant reduction in IL-17a producing cells. Taken together, we have shown that Gli3 is the only Hh transcription factor that is expressed and functionally important in Th17 cells.

Apart from its central role in canonical Hh signaling, non-canonical roles of Smo have recently emerged and Smo has been implicated as a regulator of AMPK phosphorylation in brown adipose tissue and neurons<sup>23, 26</sup>. Since AMPK has been shown to be important for promoting Th17 polarization and pathogenicity in both mouse and human<sup>27, 28</sup>, we investigated whether Smo would regulate activating AMPK phosphorylation marks in Th17 cells. To this end, we analyzed Hh-inhibited and control CD4<sup>+</sup> T cells by western blot for pAMPK and observed a dose-dependent decrease of pAMPK upon Hh signaling inhibition (Fig. 7F). Furthermore, the expression of the upstream AMPK regulating kinases CaMKK2 and LKB1 was also reduced as had been previously described in adipose tissue<sup>23</sup>.

Another non-canonical signaling mode of Smo is its direct function as a GPCR<sup>24</sup>, which is highly sensitive to pertussis toxin inhibition. To investigate whether this signaling mode is important for Th17 polarization we treated naïve CD4<sup>+</sup> T cells for 5 days with pertussis toxin under Th17 polarizing conditions. Pertussis toxin treatment did not affect viability or proliferation and had no effect on IL-17a production (Fig. 7G).

Taken together, we have uncovered Gli3 as a fundamental new TF implicated in Th17 polarization that works together with non-canonical Hh signaling via pAMPK.

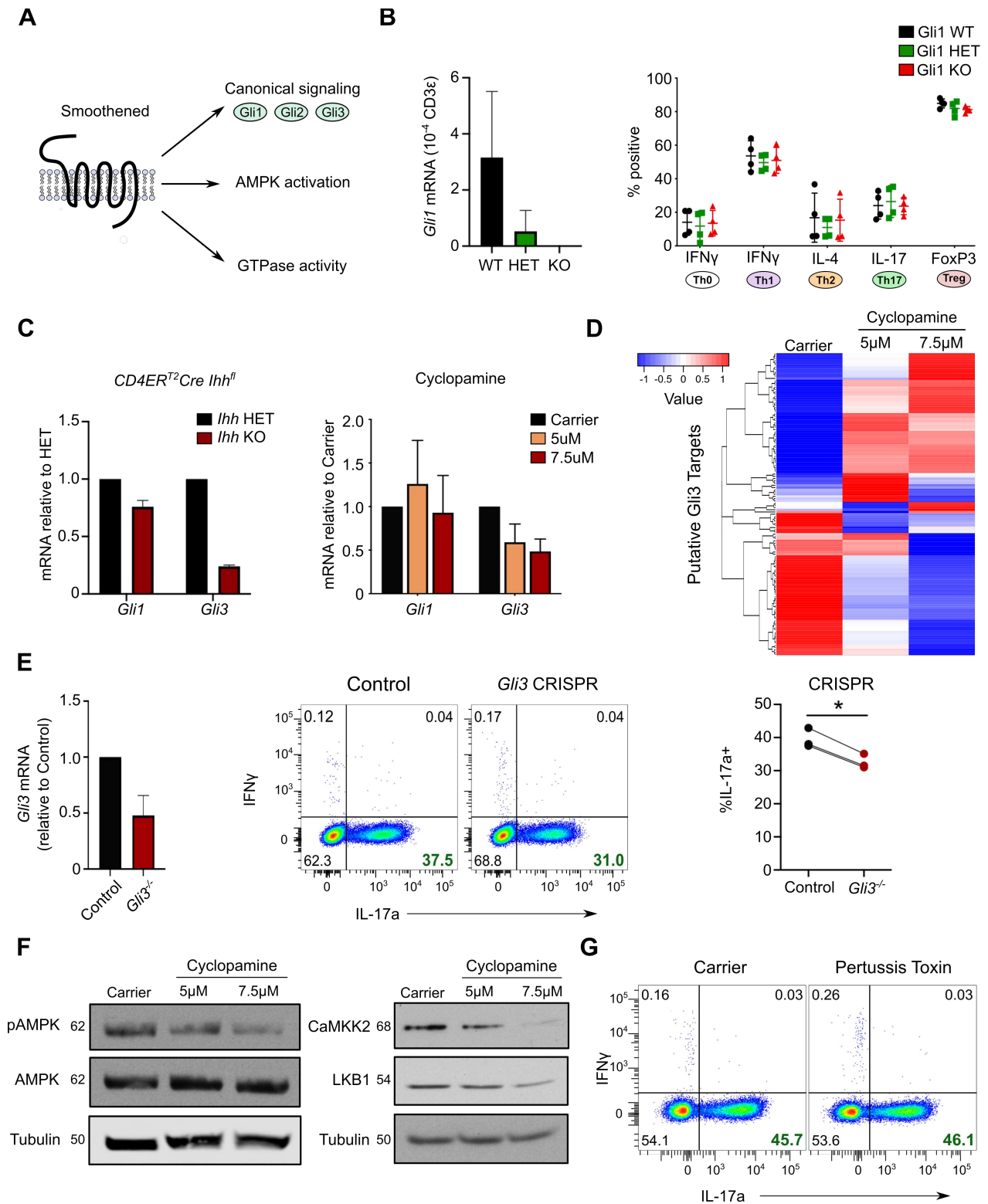


**Figure 7**

**Figure 7: Canonical and non-canonical Hh signaling contribute to Th17 polarization.** (A) Schematic overview of canonical and non-canonical Hedgehog signaling. (B) Naïve CD4<sup>+</sup> T cells were purified from spleen and peripheral lymph nodes of *Gli1eGFP<sup>+/+</sup>* (WT), *Gli1eGFP<sup>+/-</sup>* (HET) or *Gli1eGFP<sup>-/-</sup>* (KO) mice. Cells were stimulated under Th0, Th1, Th2, Th17 or Treg polarizing conditions. Cells were assessed for expression of *Gli1* RNA on day 3 (Th17, left) or harvested for analysis by flow cytometry on day 5 (right). n = 4 mice per genotype. No statistically significant differences in cytokine production were observed between genotypes. (C) Analysis of *Gli1* and *Gli3* expression by qRT-PCR of Th17 cells on day 3. Panel on the left shows Th17 cells polarized from *CD4ER<sup>T2</sup>Cre<sup>+</sup> Ihh<sup>+/fl</sup>* (HET) or *CD4ER<sup>T2</sup>Cre<sup>+</sup> Ihh<sup>fl/fl</sup>* (KO) mice. Panel on the right shows Th17 cells polarized from C57BL/6 mice in the presence of the indicated dose of cyclopamine or carrier control for three days. Data are normalized to *Tbp* as a reference gene. Similar results were obtained when *CD3ε* was used as a reference. n = 2-3 independent experiments. (D) Expression of all putative Gli3 target genes as predicted by *Miraldi et al. (2019)* in RNA-Seq analysis from Fig. 6C. Th17 cells were polarized as described above stimulated in the presence of the indicated doses of cyclopamine or carrier control for three days and harvested at day 3. Six samples/group (E-G) Naïve CD4<sup>+</sup> T cells were purified from spleen and peripheral lymph nodes of C57BL/6 mice and stimulated under Th17 polarizing conditions. (E) After 24h CRISPR/Cas9 RNP complexes targeting *Gli3* were electroporated. Cells were harvested for qRT-PCR analysis of *Gli3* at day 3 (left panel) and for analysis by flow cytometry on day 5 (middle panel). Quantitation of IL-17a expression is shown on the right. n = 3 independent experiments. (F) Naïve CD4<sup>+</sup> T cells were stimulated in the presence of the indicated doses of cyclopamine or carrier control for three days. Immunoblot analysis of Th17 cells on day 3 for pAMPK, AMPK, CaMKK2, LKB1 and Tubulin is shown. n = 3 independent experiments. (G) Naïve CD4<sup>+</sup> T cells were stimulated in the presence of 100ng/ml pertussis toxin or carrier control for five days. Cells were analyzed by flow cytometry on day 5. n = 3 independent experiments. Data are means +/- SD. p-values were calculated using an unpaired two-tailed Student's t test. \* p<0.05, \*\* p<0.01, \*\*\* p<0.001.

485 **DISCUSSION**

Our work is the first to describe that Hh signaling selectively controls Th17 polarization, but not polarization into Th1, Th2, and iTreg lineages. We show that the critical Hh pathway components Smo and Gli3 are both selectively upregulated in Th17 cells at the  
490 time of lineage determination and are induced by Th17-polarizing cytokines IL-6 and TGF $\beta$ , respectively. The TGF $\beta$ -mediated induction of Gli3 is in line with previous findings in the literature that Gli2 is a direct target of TGF $\beta$  signaling<sup>29</sup>. Ihh is the only Hh ligand expressed in Th17 cells. Furthermore, utilizing two strategies, namely CD4<sup>+</sup> T cells from a conditional CD4-specific *Ihh* KO mouse and treatment with recombinant active Ihh, we  
495 show for the first time that Hh signaling in CD4<sup>+</sup> T cells is solely driven by endogenous intracellular Ihh and does not depend on exogenous Hh ligands. This finding functionally validates and extends the previous suggestion that Hh signaling may operate intracellularly in CD8<sup>+</sup> T cells<sup>11</sup>. This novel mode of signaling might present a unique characteristic of the Hh pathway in lymphocytes to ensure that signaling is independent  
500 of fluctuating exogenous ligand gradients.

We identify Gli3 as a novel transcription factor that controls Th17 lineage polarization. Our observation functionally validates an ATACSeq-based bioinformatic model that suggested Gli3 is part of the top 30 “core” TFs of the Th17 transcriptional regulatory  
505 network<sup>19</sup>. We show that Hh-induced Gli3 regulates the transcription of previously predicted Gli3 target genes (Suppl. Fig. 10) known to control Th17 polarisation<sup>19</sup>. This crucial role for Gli3 seems to be restricted to CD4<sup>+</sup> T cells, since Gli3 expression has not been reported in CD8<sup>+</sup> T cells<sup>11</sup>.

Furthermore, we show that Hh signaling influences the metabolic regulation of Th17 cells  
510 through a known non-canonical Hh signaling axis via CaMKK2/LKB1 and pAMPK in adipose tissue<sup>23</sup>. This is in line with published data indicating a role of pAMPK in human and murine Th17 polarization<sup>27, 28</sup> and in the pathogenicity of Th17 cells in a model of adoptive T cell transfer colitis<sup>27</sup>.

Our model is summarized in Suppl. Fig. 11.

515

Hh signaling has been implicated in CD4<sup>+</sup> T cell polarization of Th2 but not Th1 cells<sup>12</sup>. Furmanski *et al* used mice expressing transgenic Gli2A (activator) or Gli2R (repressor) and showed an effect of exogenous Shh on Th2 differentiation. Our findings that Gli2 transcripts are absent in murine Th cultures and that Th17 cells do not respond to exogenous lhh ligand might resolve these differences. In addition, it has been shown that exogenous recombinant Shh is unable to induce Th17 polarization in human CD4<sup>+</sup> T cells<sup>30</sup> supporting our model of a unique intracellular Hh signaling pathway in T lymphocytes.

Th17 cells show remarkable plasticity compared to other Th subsets due to their stem cell potential. Depending on the microenvironment, Th17 cells have the ability to convert into nearly all other CD4<sup>+</sup> Th lineages<sup>21</sup>. This phenomenon is particularly well studied in autoimmune disease, cancer and infection where Th17 cell conversion into Th1 cells is critical for the overall CD4 effector response<sup>22, 31</sup>. Hh signaling is functionally important for the maintenance of various stem cell compartments throughout the body, as well as cancer stem cells<sup>32, 33, 34, 35, 36</sup> and it remains to be seen whether Hh signaling can provide Th17 cells with stem cell potential in addition to being crucial for Th17 polarization. Intriguingly, we see that cells treated with Hh inhibitors lose expression of stem-cell-associated Wnt target genes *Lef1*, *Tcf4*, *Tcf7l1*, *Ascl2*, as well as *Tcf7* which was identified as the main marker of Th17 stemness (Fig. 6C)<sup>22</sup>.

Due to the central role that pathogenic Th17 cells play in numerous autoimmune diseases, including inflammatory bowel disease, rheumatoid arthritis, multiple sclerosis and psoriasis<sup>37</sup>, there has been great interest in developing therapeutic interventions that specifically target Th17 polarization and pathogenicity. The importance of Th17 cells in COVID-19 pathogenesis has further increased this interest<sup>38, 39</sup>.

There is a shortage of small molecule inhibitors that target Th17 polarization and effector function. A seminal drug screen for Ror $\gamma$ t antagonists identified digoxin as a potent inhibitor able to suppress Th17 responses *in vitro* and *in vivo*<sup>40</sup>. More recently, bromodomain inhibitors JQ1 and MS402 were found to block Th17 differentiation in pre-clinical models of intestinal inflammation<sup>41, 42</sup>. However, the extremely narrow therapeutic window of digoxin and the broad-ranging effects of targeting epigenetic regulators with

bromodomain inhibitors make their use in the clinic difficult. Here, we present data showing that clinically approved Hh inhibitor vismodegib specifically and potently inhibits Th17 polarization *in vivo*, opening up the possibility of treating autoimmune diseases with Hh inhibitors.

## 555 MATERIALS AND METHODS

### Mice

RAG2KO were a generous gift from Suzanne Turner (University of Cambridge) and OTI mice were purchased from the Jackson Laboratory (C57BL/6-Tg(TcraTcrb)1100Mjb/j, Stock no. 003831). OTI RAG2KO mice were generated from these. *Gli1-eGFP* mice were a generous gift from Alexandra Joyner (Sloan Kettering Institute)<sup>43</sup> and were backcrossed onto the C57BL/6J background (The Jackson Laboratory, Bar Harbor, ME) for more than 11 generations. *dLckCre* and *ROSA26tdTom* mice were a generous gift from Randall Johnson and Douglas Winton (University of Cambridge), respectively. *Smo<sup>ff</sup>* (Stock no. *Smo<sup>tm2Amc</sup>/J*, 004526), *Ihh<sup>f/+</sup>* (*Ihh<sup>tm1Blan</sup>/J*, Stock no. 024327) and *CD4CreERT<sup>2</sup>* (Tg(Cd4-cre/ERT2)11Gnri, Stock no. 022356) mice were purchased from The Jackson Laboratory. *Smo<sup>ff</sup>* mice were back-crossed to the C57BL/6J background (Charles Rivers Inc., UK) for more than 10 generations and crossed to *ROSA26tdTom* and *CD4CreERT<sup>2</sup>* mice to generate *CD4CreERT<sup>2</sup>/ROSA26tdTom/Smo<sup>ff</sup>* mice or with *dLckCre* mice to generate *dLckCre/ROSA26tdTom/Smo<sup>ff</sup>* mice. *Ihh<sup>ff</sup>* mice were crossed onto *CD4CreERT<sup>2</sup>/ROSA26tdTom* mice. Mice were genotyped using Transnetyx, maintained at the CRUK Cambridge Institute/ University of Cambridge, and used at 6-8 weeks of age. All housing and procedures were performed in strict accordance with the United Kingdom Home Office Regulations.

575

### Murine CD4 *in vitro* polarization

Spleens were harvested and placed into ice-cold sterile DPBS (Gibco, cat no. 14190094, hereafter referred to as PBS). Spleens were dissociated through a 70  $\mu$ m filter (Greiner, cat no. 542070) using the top of the plunger from a 2 ml syringe. Filters were washed with ice-cold, sterile MACS Buffer, made with PBS + 2% fetal calf serum (FCS, Biosera, cat no. 1001, 500ml) + 2 mM EDTA and then centrifuged at 1200 rpm for 10 min at 4°C. Naïve murine CD4<sup>+</sup> T cells were isolated using a negative-selection MACS approach (Naïve CD4<sup>+</sup> T Cell Isolation Kit, cat no. 130-104-453, Miltenyi Biotec). MACS separation was performed by loading the labelled cell suspension through a 50 $\mu$ m sterile CellTrics Partec filter (Wolflabs, cat no. 04-004-2327) onto the LS column (Miltenyi Biotec, cat no. 130-042-401). The purity of the sorted populations was above 95%.

CD4<sup>+</sup> T cells were plated onto a 96-well plate pre-coated overnight at 4°C with 2.5  $\mu$ g/ml anti-CD3 $\epsilon$  and 2  $\mu$ g/ml anti-CD28 antibody (Table 4). For Th polarization experiments CD4<sup>+</sup> T cells were plated at a final concentration of 1x10<sup>6</sup> cells/ml in complete IMDM supplemented with cytokines/blocking antibodies to induce lineage polarization

Lineage	Cytokine/ Blocking Antibody	Final concentration	Cat no.	Supplier
Th0	IL-2	20ng/ml	200-02-500	Peprotech
Th1	IL-12	4ng/ml	210-12-10	Peprotech
	Anti IL-4	5 $\mu$ g/ml	504115	Biologend
Th2	IL-4	10ng/ml	214-14-50	Peprotech
	Anti IFN $\gamma$	10 $\mu$ g/ml	517904	Biologend
Th17	IL-1 $\beta$	10ng/ml	211-11B-50	Peprotech
	IL-6	20ng/ml	216-16-50	Peprotech
	IL-23	10ng/ml	1887-ML	R&D Systems
	TGF $\beta$	1ng/ml	100-21-50	Peprotech
	Anti IL-4	5 $\mu$ g/ml	504115	Biologend
	Anti IFN $\gamma$	10 $\mu$ g/ml	517904	Biologend
iTreg	IL-2	20ng/ml	200-02-500	Peprotech
	TGF $\beta$	10ng/ml	100-21-50	Peprotech
	Anti IL-4	5 $\mu$ g/ml	504115	Biologend
	Anti IFN $\gamma$	10 $\mu$ g/ml	517904	Biologend

Table 1: Murine polarizing cytokines used for CD4<sup>+</sup> Th cell polarization

595

### **Cell Culture**

Purified naïve CD4<sup>+</sup> T cells were resuspended in IMDM (Gibco, cat no. 12440-053) supplemented with 5% heat-inactivated batch-tested FCS (Biosera, cat no. 1001-500ml), 10 µM β-Mercaptoethanol (50mM, Gibco, cat no. 31350-010) and 100 U/ml  
600 Penicillin/Streptomycin (10'000 U/ml, Gibco, cat no.15140-122).

*Smo* KO mouse embryonic fibroblasts (MEFs) were generated by James Chen (Stanford University) and kindly provided by Natalia A Riobo-Del Galdo (University of Leeds). WT MEFs were a generous gift from Jane Goodall (University of Cambridge). MEFs were cultured in DMEM medium (DMEM, Gibco, cat no. 10566-016; 500 ml) supplemented  
605 with 10% heat-inactivated, batch-tested FCS (Biosera, cat no., 1001) and 100 U/ml penicillin/streptomycin (Gibco, cat no. 15140-122; 10,000 U/ml). All cell lines tested mycoplasma negative (MycoProbe<sup>®</sup> Mycoplasma Detection Kit, R&D systems). Cells were grown in a humidified incubator at 37°C and 5% CO<sub>2</sub>.

610

### **CRISPR of primary naïve CD4<sup>+</sup> T cells**

Alt-R<sup>®</sup> CRISPR-Cas9 crRNA (IDT) and tracrRNA (IDT, cat no. 1072534) were reconstituted at 100 µM in nuclease-free duplex buffer (IDT). 1.9 µl of each stock solution was mixed with 8.7 µl duplex buffer. Samples were heated in a thermal cycler at 95°C for  
615 5 min and left for 10 min at room temperature. 10.5 µl Buffer T (Thermo, cat no. MPK10096) was added as well as 2 µl TrueCut™ Cas9 Protein v2 (5mg/ml, Thermo, cat no. A36499) which was pipetted very slowly in a circular motion to ensure optimal solubility. The mixture was incubated at 37°C for 10 min to assemble the ribonucleoprotein (RNP) complex.

620 Naïve CD4<sup>+</sup> T cells were isolated from C57BL/6 spleens and stimulated with plate bound anti-CD3ε/CD28 antibodies in the presence of Th17 polarizing cytokines as described previously. After 24 h of stimulation, cells were washed twice in pre-warmed PBS (Gibco) prior to resuspension in 80 µl Buffer T (1 million cells/electroporation reaction). The suspension was briefly mixed with the RNP complex solution prior to electroporation with  
625 the Neon™ electroporation system in 100 µl electroporation tips (Thermo, cat no.

MPK10096) with three pulses of 1600 V each with a pulse width of 10 ms. Cells were left to recover in complete IMDM in the absence of antibiotics for 20 min. Cells were then centrifuged at 1500 rpm for 5 min and returned into culture to an anti-CD3 $\epsilon$ /CD28 antibody coated plate in complete IMDM (without antibiotics) supplemented with polarizing cytokines at the concentrations mentioned previously. Cells were centrifuged at 1000 rpm for 1 min for quick adherence to the coated plate. Antibiotics were re-added after six hours at the indicated concentrations.

*Gli3* was targeted with two crRNA sequences:

Guide 1: 5'-GCATATGAGAAGACACACTG-3'

635 Guide 2: 5'-CTCTCATCACTAGACGTCGA-3'

Two non-targeting crRNA sequences were used for the negative control (IDT, cat no. 1072544/10725455). Indels were validated using the Alt-R Genome Editing Detection Kit (IDT, cat no. 1075932) per the manufacturer's instructions.

#### 640 ***In vivo* tamoxifen treatment**

75 mg/kg/day of tamoxifen (Sigma, cat no. T5648) prepared in 100  $\mu$ l of a 10% ethanol (Sigma, cat no. E7023), 90% corn oil (Sigma, cat no. C8267, autoclaved) solution. Tamoxifen was prepared by adding ethanol, then corn oil and sonicating for 30 min in a 37°C water bath. Tamoxifen solution was given to the mice once a day for 4 consecutive days as an intraperitoneal injection.

#### **Flow cytometry and cell sorting**

##### *Surface staining*

Cells were stained in 96-well round-bottom plates (Corning) or 5 ml polystyrene round bottom tubes (Fisher Scientific/Falcon, cat no. 352003). Samples were washed twice with ice-cold PBS and incubated for 10 min light protected at room temperature with Fixable Viability dye eFlour780, prepared at 1:1000 in PBS (eBioscience, cat no. 65-0865-18; 500 tests). Cells were then washed once with FACS buffer, made with PBS (Gibco, cat no. 14190094) + 3% FCS (Biosera) + 0.05% Sodium Azide (Sigma, cat no. 71289), + 2 mM EDTA (prepared in-house). Cells were then incubated with Fc block (1:100; Biolegend TruStain fcX anti-mouse CD16/32, cat no. 101320) for 5 min at room temperature protected from light. Next, cells were incubated with 50  $\mu$ l of fluorophore-conjugated

antibodies at the appropriate dilution (Table 1) for 20 min at 4°C protected from light. Cells were washed twice with FACS buffer and moved to 5 ml polystyrene round bottom tubes prior to immediate analysis (Fisher Scientific/Falcon) or fixation for intracellular staining.

660 *Intracellular staining*

For the staining of intracellular cytokines, cells were incubated at 37°C for 4h in the presence of 1 µg/ml Ionomycin (Sigma, cat no. I9657) and 50 ng/ml PMA (Sigma, cat no. P1585) and Golgistop (BD, Cat no. 554724) added for the duration of stimulation per the manufacturer's instructions. Following surface marker staining (as above), cells were  
 665 fixed with BD Cytotfix/Cytoperm Plus Fixation Buffer (BD Biosciences, cat no. 554715) for 25 min at 4°C protected from light. Samples were then spun down in a table-top centrifuge and washed once with permeabilization buffer (10x; BD Biosciences, cat no. 554715), prepared to a final concentration of 1x with Milli-Q Water (in-house). Cells were resuspended in 50 µl of permeabilization buffer containing fluorophore-conjugated  
 670 antibodies at the appropriate concentration (Table 1) and incubated light protected at 4°C for 30 min. Prior to analysis, cells were washed once in permeabilization buffer and once in FACS buffer.

Flow cytometric analyses were conducted on a BD LSR II or BD LSR Symphony cell  
 675 analyzer in the presence of AccuCheck counting beads (Thermo Fisher, Cat no. PCB1000) where indicated, and data was analyzed with FlowJo software (Tree Star Inc., version 10.4).

Target	Clone	Reactivity	Fluorochrome	Dilution	Cat no.	Supplier
CCR6	140706	Mouse	BUV395	1:100	747831	BD
CD3ε	145-2C11	Mouse	BUV395	1:50	583565	BD
CD4	RM4-5	Mouse	BV605	1:200	100548	Biolegend
CD4	RM4-5	Mouse	APC	1:200	100516	Biolegend
CD8a	53-6.7	Mouse	BV605	1:200	100744	Biolegend
CD8a	53-6.7	Mouse	PE	1:200	100707	Biolegend
CD8a	53-6.7	Mouse	BUV396	1:200	563786	BD
CD44	IM7	Mouse/Human	BV785	1:400	103059	Biolegend
CD45	30-F11	Mouse	Alexa Fluor 488	1:200	103122	Biolegend
CD45	30-F11	Mouse	PE/Cy7	1:200	103114	Biolegend
CD62L	MEL-14	Mouse	BV421	1:200	104436	Biolegend

CD90.1	HIS51	Mouse/Rat	APC	1:200	17-0900-82	BD
CD90.2	53-2.1	Mouse	PE	1:200	140308	Biolegend
TCR $\beta$	H57-597	Mouse	BV711	1:200	109243	Biolegend
TCR $\gamma\delta$	GL3	Mouse	Alexa Fluor 488	1:200	118128	Biolegend
IL-4	11B11	Mouse	APC	1:100	504106	Biolegend
IL-4	11B11	Mouse	BV711	1:100	504133	Biolegend
IL-10	JES5-16E3	Mouse	PE/Cy7	1:100	505025	Biolegend
IL-17a	TC11-18H10.1	Mouse	BV421	1:100	506925	Biolegend
IL-22	IL22JOP	Mouse	APC	1:100	17-7222-82	Thermo Fisher
IFN $\gamma$	XMG1.2	Mouse	BV711	1:100	505835	Biolegend
IFN $\gamma$	XMG1.2	Mouse	APC	1:100	505810	Biolegend
IFN $\gamma$	XMG1.2	Mouse	PE/Cy7	1:100	505826	Biolegend
FoxP3	FJK-16S	Mouse/Rat	APC	1:100	17-5773	eBioscience
T-bet	4B10	Mouse/Human	PE/Cy7	1:100	644824	Biolegend
pSTAT3 Y705	4/P-STAT3	Mouse/Human	Alexa Fluor 647	1:100	557815	BD

Table 2: Antibodies used for flow cytometry experiments

680

### ***In vitro* Hh inhibitor/ligand treatment**

CD4<sup>+</sup> T cells were treated with the Smo inhibitors cyclopamine (Alfa Aesar, cat no. J61528; 25 mg) or vismodegib (LC Laboratories) at the concentrations indicated. Stock solutions were prepared in DMSO (Life Technologies) for vismodegib and ethanol for cyclopamine at 10 mM and diluted to working concentration in complete IMDM (Gibco). Vismodegib stocks were prepared from fresh vials and used within a week. For Ihh treatment, CD4<sup>+</sup> T cells were treated with recombinant N-terminal Ihh peptide (R&D Systems, Cat. No. 1705-HH-025/CF) per the manufacturer's instructions at the concentrations indicated.

690

### **qRT-PCR**

Cells harvested for RNA extraction were washed twice in ice-cold PBS, snap-frozen as dry pellets, and stored at -80°C. RNA was extracted using the RNAqueous™-Micro Total RNA Isolation Kit according to the manufacturer's instructions. RNA concentration was measured with a Nanodrop spectrophotometer (Labtech ND-1000) and samples were stored at -80°C if not used immediately.

Reactions for qRT-PCR were set up in 384 well plate format on ice at a final volume of 10  $\mu$ l using the One-Step qRT-PCR Kit (Thermo Fisher SuperScript III Platinum, cat no.

11732088). The reaction contained 5  $\mu$ l 2x Reaction mix, 3  $\mu$ l total RNA, 0.5  $\mu$ l 20x  
 700 Taqman probe (Thermo Fisher, see Table 2), 0.2  $\mu$ l Superscript III RT/Platinum Taq  
 enzyme, and 1.3  $\mu$ l nuclease-free ddH<sub>2</sub>O.

Probe	Cat no.	Exon Boundary
<i>CD3<math>\epsilon</math></i>	Mm00599684_g1	6-7
<i>Tbp</i>	Mm00446973_m1	4-5
<i>Dhh</i>	Mm01310203_m1	1-2
<i>Shh</i>	Mm00436528_m1	2-3
<i>Ihh</i>	Mm01259021_m1	1-2
<i>Smo</i>	Mm01162710_m1	8-9
<i>Ptch1</i>	Mm00436026_m1	17-18
<i>Ptch2</i>	Mm00436047_m1	19-20
<i>Gli1</i>	Mm00494654_m1	11-12
<i>Gli2</i>	Mm01293111_m1	13-14
<i>Gli3</i>	Mm00492345_m1	14-15
<i>Il17a</i>	Mm00439618_m1	1-2
<i>Runx1</i>	Mm01213404_m1	6-7
<i>Rora</i>	Mm01173766_m1	9-10
<i>Rorct</i>	Mm01261022_m1	5-6
<i>Batf</i>	Mm00479410_m1	1-2
<i>Irf4</i>	Mm00516431_m1	5-6
<i>Vax2</i>	Mm00496315_m1	1-2

Table 3: Probes used for qRT-PCR

705 Each sample was run in triplicate with *Tbp* and *CD3 $\epsilon$*  used as housekeeping genes. In  
 addition, each experiment included a non-template control and each probe was validated  
 by a non-RT control where Platinum Taq DNA Polymerase (Life Tech, cat no. 10966018)  
 was used instead of SuperScript Platinum III RT. Samples were run on a QuantStudio 6  
 710 Flex Real-Time PCR System (Thermo Fisher). Reverse transcription thermal cycling was  
 set at 50°C for 15 min, followed by 2 min at 95°C and 45 cycles of PCR with 15 sec at  
 95°C, then 1 min at 60°C.

Expression of the gene transcript of interest was calculated with the  $\Delta$ Ct method  
 (Schmittgen and Livak, 2008). The cycle threshold (Ct) value from the gene of interest  
 715 was subtracted from the housekeeping gene and transformed with a factor of  $2^{(-\Delta Ct)}$  to  
 give the fold expression relative to the housekeeping gene.

## Monoclonal antibody generation

720 PCR was used to amplify cDNA encoding the C-terminal 248 amino acids of *mus musculus* Smo (aa 545 -793) followed by a 6xHis tag. The PCR product was cloned into the BamH1 and EcoR1 sites of the pGEX-4T1 vector (GE Healthcare) by Gibson assembly (New England Biolabs). Expression of the GST-Smo C-terminal-6xHis tag fusion protein (GST-CSmoHis) was carried out in the host *E. coli* strain SHuffle® T7 *E.coli*/K12 overnight at 16°C. The cell culture (4 L) was harvested by centrifugation at 725 4000g for 10 minutes and the pellet was resuspended in 50 mM phosphate buffer pH 7.5 containing 150 mM NaCl (PBS) and lysed in an Avestin EmulsiFlex C5 homogenizer. The lysate was clarified by centrifugation at 48,000 g for 30 min and the supernatant applied to a column containing 2.5 ml packed volume of glutathione-Sepharose (GE Healthcare). The column was washed extensively with PBS and GST-CSmoHis was eluted with 730 mM glutathione. The eluate was then treated with 20 U of Thrombin (Sigma-Aldrich) for 5 hours at room temperature and loaded onto a column containing 0.5 ml packed volume of Ni NTA affinity resin. After extensive column washing, the CSmoHis protein was eluted with PBS containing 350 mM imidazole, desalted and concentrated to a concentration of 1 mg/ml protein.

735 The fusion was made from splenocytes of NMRI mice or SPRD rats (Taconic), which were SC immunized twice at a 14-day interval with 30 µg of the murine Smo C-terminal part aa544-793 containing a 6xHIS tag antigen glutaraldehyde coupled to diphtheria toxoid. The antigen was administered with the GERBU P™ adjuvant according to the manufacturer's recommendations. Four days prior to the fusion, the animals received an 740 IV injection boost of 15 µg antigen administered with adrenaline.

Fusions and screenings were essentially performed as described before with the mouse SP2 myeloma cell line as the fusion partner <sup>44</sup>.

## Immunofluorescence

745 WT and Smo KO MEFs were grown on coverslips to confluency. Primary murine cells  
were diluted to  $1 \times 10^6$  cells/ml, plated onto glass slides and allowed to adhere to the glass  
at 37°C for 10 min. Cells were fixed with 4% PFA (16% PFA solution, CN Technical  
Services, cat no. 15710-s, 1x PBS (from 10x PBS, in-house), and Milli-Q H<sub>2</sub>O) for 10 min  
at room temperature. Slides were washed 5 times with PBS (in-house) and blocked with  
750 blocking buffer: PBS + 1% bovine serum albumin (BSA, Sigma, cat no. A3912; 50 g  
lyophilized powder) + 0.1% TritonX-100 (Alfa Aesar) for 30 min at room temperature.  
Blocking solution was aspirated and mouse (Clone 18-2-3) Smo hybridoma supernatant  
+ 0.1% TritonX-100 was added. Slides were incubated for 1.5 hours at room temperature  
and then washed 5 times with PBS + 0.1% TritonX-100. Anti-mouse AlexaFlour 488  
755 secondary (Thermo, cat no. A21202, 1:500 dilution) was added in blocking buffer (PBS +  
1% BSA + 0.1% TritonX-100) and slides were incubated for 30 min, at room temperature  
and protected from light. After incubation, slides were washed 5 times with PBS + 0.1%  
TritonX-100 and stained with Hoechst (Hoechst 33342, trihydrochloride, trihydrate  
Invitrogen/Fisher, cat no. H3570, 1:30,000 dilution) prepared in PBS for 5 min, light  
760 protected at room temperature. Slides were washed 5 times with PBS and mounted with  
ProLong Diamond Antifade Mountant (Fisher, cat no. P36961). Excess mounting fluid  
was wiped off and slides were allowed to set at room temperature and light protected  
overnight before imaging.

#### 765 **Image acquisition and analysis**

Confocal spinning disc microscopy was performed on an Andor Dragonfly 500 (Oxford  
Instruments). Images were processed using Imaris software (Bitplane/Oxford  
Instruments).

#### 770 **Western Blot**

Cells were harvested at 4°C, washed twice in ice-cold PBS and lysed in ice-cold RIPA  
buffer (150mM NaCl, 50mM Tris-HCl pH 8.0, 1mM MgCl<sub>2</sub>, 2% Triton) with protease  
inhibitor (Pierce, cat. No. 88666) at a concentration of  $40 \times 10^6$  cells/ml for 15 min on ice  
with intermittent vortexing. PhosStop phosphatase inhibitor (Sigma, cat No. 4906845001)  
775 was added in the lysis buffer for samples where phosphoepitopes were to be detected.

780 Lysates were centrifuged at 13'000 rpm for 10 min at 4°C and the supernatant was transferred to a fresh tube and stored at -80°C. Samples were boiled (100°C) for 3 min or incubated at 37°C for 15min where Smo was to be probed, and loaded, together with a protein standard (Bio Rad, cat no. 161-0394) onto a NuPAGE 4-12% gradient Bis/Tris Acrylamide gel (Thermo Fisher, cat no NP0335BOX). PAGE was run in Nu-PAGE MOPS running buffer (Thermo Fisher, cat no. NP0001). Western blotting was performed using wet transfer in Nu-PAGE Transfer Buffer (Thermo Fisher, cat no. NP0006-01) + 10% Methanol (Honeywell, cat no. 32213-2.5L) for 90 min at room temperature at 300 mA constant onto a 0.45 µm nitrocellulose membrane (Thermo Fischer, cat no LC2001).  
 785 Membranes were blocked with 5% (w/v) nonfat dry milk (Marvel Original, Dried Skimmed Milk) in TBST or in 5% BSA in TBST for 1 h at room temperature prior to overnight incubation with primary antibody at 4°C. The membrane was developed with SuperSignal West Pico Plus Chemiluminescent Substrate (Thermo Fisher, cat no. 34580) or SuperSignal West Dura Extended Duration Substrate (Thermo Fisher, cat no. 34075)

790

Target	Clone	Reactivity	Type	Dilution	Cat no.	Supplier
Actin	AC-40	Mouse anti-human/rat/mouse	Primary	1:1'000	A3853	Sigma
AMPK $\alpha$	N/A	Rabbit anti-human/rat/mouse	Primary	1:1'000	2532	Cell Signaling
pAMPK $\alpha$ Thr172	40H9	Rabbit anti-human/rat/mouse	Primary	1:1'000	2535	Cell Signaling
CaMKK2	D8D4D	Rabbit anti-human/rat/mouse	Primary	1:1'000	16810	Cell Signaling
LKB1	D60C5	Rabbit anti-human/rat/mouse	Primary	1:1'000	3047	Cell Signaling
Ptch	Polyclonal	Rabbit anti-human/mouse	Primary	1:1'000	ab53715	Abcam
Smoothened	18-10-10	rat	Primary	1:5 hybridoma supernatant	N/A	N/A
$\alpha$ -tubulin	DM1A	Mouse anti-human/rat/mouse	Primary	1:2'000	3873	Cell Signaling
	Polyclonal	Goat anti-mouse	Secondary (HRP conj.)	1:15'000	P0447	Dako
	Polyclonal	Donkey anti-rabbit	Secondary (HRP conj.)	1:10'000	P0448	Dako
	Polyclonal	Goat anti-rat	Secondary (HRP conj.)	1:3'000	7077S	Cell Signaling

Table 4 : Antibodies used for western blot

## 795 **RNA Sequencing**

Samples were generated and RNA was extracted as previously described. Six biological replicates were used per condition. RNA quality was assessed using a capillary electrophoresis system (4200 TapeStation, Agilent) using RNA ScreenTape (Agilent, cat no. 5067-5576) as per the manufacturer's instructions. RNA concentrations were  
800 quantified using the Qubit™ RNA BR Assay kit (Thermo, cat no. 10210) as instructed by the manufacturer. Libraries were generated using the TruSeq stranded mRNA kit (Illumina) following the manufacturer's instructions and sequenced using single-read sequencing with the HiSeq4000 platform (Illumina).

805 Reads were aligned to the mouse genome version GRCm38 using STAR v2.5.3a<sup>45</sup>. Read counts were obtained using feature Counts function in Subread v1.5.267<sup>46</sup> and read counts were normalized and tested for differential gene expression using the DESeq2 workflow<sup>47</sup>. Multiple testing correction was applied using the Benjamini–Hochberg method.

810 Gene Set Enrichment Analysis (<http://www.broad.mit.edu/gsea>) was carried out using the gene sets from Molecular Signatures Database (MSigDB)<sup>48</sup>. Genes were ranked based on the log<sub>2</sub> Fold change multiplied by  $-\log_{10}(\text{padj})$ .

815

## **CD3 injection model of small intestinal inflammation**

8-10-week-old female C57BL/6 mice were injected with 20µg anti-CD3 monoclonal antibody (Clone: 145-2C11) at 0h and 48h as previously described<sup>16</sup>. Mice were dosed  
820 every 12h by oral gavage with 100mg/kg vismodegib (LC laboratories), prepared in MCT from a fresh vial for each experiment (0.5% methylcellulose, 0.2% Tween 80), or carrier control, with four to five mice per group. Mice were harvested at 52h, at which point serum was collected and small intestines were harvested in ice-cold PBS. Small intestines were cleaned using ice-cold PBS, cut into roughly 5 mm pieces and collected in complete  
825 IMDM. Tissue pieces were rotated for 30 min at room temperature to release

intraepithelial lymphocytes (IELs). Cells were strained on a 70 µm filter and IELs were collected from the interface of a 40%-80% Percoll gradient (GE Healthcare, cat no. 17089101). IELs were restimulated for 4h with PMA and Ionomycin in the presence of Monensin and subjected to viability, surface and intracellular flow cytometric staining (for details see section on flow cytometric methods). Serum IL-17a concentrations were determined using the ELISA MAX™ Deluxe Set Mouse IL-17A (Biolegend, cat no. 432504) according to the manufacturer's instructions.

835

### **Adoptive T cell transfer colitis model**

CD4<sup>+</sup> T cells were isolated from spleen and peripheral lymph nodes of donor mice as described previously using MACS isolation. The CD4<sup>+</sup> T cells were stained in MACS Buffer for 15min at 4°C for CD4, CD25, CD45RB and DAPI was added prior to FACS sorting which was performed as described above. Pure CD4<sup>+</sup> CD25<sup>-</sup> CD45RB<sup>hi</sup> tdTomato<sup>+</sup> cells were sorted to high purity. Cells were washed twice in PBS prior to intraperitoneal injection into Rag2<sup>-/-</sup> recipient mice. A cell suspension of 200 µl at 2x10<sup>6</sup> cells/ml PBS were injected intraperitoneally per mouse. Mice were weighed at least twice weekly thereafter and harvested between 5-6 weeks after injection.

Colons, mesenteric lymph nodes and spleens were harvested in sterile ice-cold PBS. Colons were flushed through with ice-cold PBS to remove faeces and a 5-10 mm representative sample was collected in 10% Neutral Buffered Formalin (NBF). These samples were incubated overnight in NBF prior to being moved to a 70% Ethanol solution for H&E staining (in-house histopathology core). After collection of histology samples, the colon was cut into roughly 5mm pieces collected in a 50 ml falcon with complete IMDM + 58 µg/ml DNase (Stem Cell Technologies, cat no. 7469) + 58 µg/ml Liberase, Thermolysin low (Roche, cat no. 5401020001) and incubated in a shaker at 37°C for 25 min at 225 rpm to release colonic lamina propria lymphocytes (LPLs). Cells were strained twice through a 70 µm filter and LPLs were collected from the interface of a 40%-80% Percoll gradient (GE Healthcare, cat no. 17089101). Spleens were mashed through a 70

860  $\mu\text{m}$  filter with sterile PBS and collected from the interface of a Lympholyte gradient (Cedarlane Laboratories, cat no. CL5035). Gradient centrifugations were set up in 15 ml falcons and centrifuged for 1800 rpm for 20 min (acceleration 1/9, deceleration 0/9). Mesenteric lymph nodes were strained twice on a 40  $\mu\text{m}$  filter.

865 LPLs, splenocytes and lymph node suspensions were restimulated for 4 h with PMA and Ionomycin in the presence of Monensin and subjected to viability, surface and intracellular flow cytometric staining (for details see section on flow cytometric methods). Statistical analysis was performed using Prism 7 software (GraphPad Inc.). Statistical analysis was performed using an unpaired two-tailed Student's t test or Mann Whitney U test, respectively. For each data set, the presence of a statistically significant outlier was assessed using Grubbs' test ( $\alpha = 0.05$ ) and where present was excluded from subsequent  
870 analysis.

875 Semi-quantitative analysis of colitis severity was determined on formalin-fixed, paraffin-embedded and hematoxylin & eosin stained sections as similarly described <sup>49</sup>. Sections were analyzed in a blinded fashion by an independent expert. The sum of each subscore of mononuclear infiltration (0-3), crypt hyperplasia (0-3), epithelial injury (0-3), neutrophil infiltration (0-3) and inflammatory penetration (0-2) depicted colitis severity.

## **ACKNOWLEDGEMENTS**

880 Special thanks and gratitude go to Kamal Kishore and Jing Su from the Bioinformatics core at the CRUK Cambridge Institute for their support in analyzing RNASeq data; Ellie Pryor, Nicky Jacobs and Gemma Cronshaw from the BRU for expert animal care; the Histology core for processing and staining of colon samples; the flow cytometry core for assistance with cell sorting and the Genomics core for sequencing.

885 We thank Gitta Stockinger and Gillian Griffiths for advice and support on the manuscript.

This work was supported by Cancer Research UK (MdlR (A22257), H-CC, VC); Sir Henry Dale Fellowship jointly funded by the Wellcome Trust and the Royal Society (MdlR

(WT107609); LMOB); Gates Cambridge Trust (AK); JH is undertaking a PhD funded by  
890 the Cambridge School of Clinical Medicine, Frank Edward Elmore Fund and the Medical  
Research Council's Doctoral Training Partnership (award reference: 1954837)

895

### AUTHOR CONTRIBUTIONS

MdIR and JH conceived the project and designed the experiments. JH executed all  
experiments. LOB, CK, H-CC, VC and AK helped with experiments and technical  
900 expertise. Monoclonal antibodies against murine Smo were generated by KS, MS, and  
MarcdIR. TA scored the adoptive colitis model. JH and MdIR analyzed the results and  
wrote the manuscript.

### REFERENCES

905

1. Jiang, S. & Dong, C. A complex issue on CD4(+) T-cell subsets. *Immunol Rev* **252**, 5-11 (2013).
2. Zhu, J., Yamane, H. & Paul, W.E. Differentiation of effector CD4 T cell populations (\*).  
910 *Annu Rev Immunol* **28**, 445-489 (2010).
3. Ivanov, II *et al.* The orphan nuclear receptor ROR $\gamma$  directs the differentiation program of proinflammatory IL-17+ T helper cells. *Cell* **126**, 1121-1133 (2006).
4. Ciofani, M. *et al.* A validated regulatory network for Th17 cell specification. *Cell* **151**,  
915 289-303 (2012).
5. Stockinger, B. & Omenetti, S. The dichotomous nature of T helper 17 cells. *Nat Rev Immunol* **17**, 535-544 (2017).
6. Goetz, S.C. & Anderson, K.V. The primary cilium: a signalling centre during vertebrate  
920 development. *Nat Rev Genet* **11**, 331-344 (2010).
7. Briscoe, J. & Therond, P.P. The mechanisms of Hedgehog signalling and its roles in  
925 development and disease. *Nat Rev Mol Cell Biol* **14**, 416-429 (2013).

8. Crompton, T., Outram, S.V. & Hager-Theodorides, A.L. Sonic hedgehog signalling in T-cell development and activation. *Nat Rev Immunol* **7**, 726-735 (2007).
- 930 9. Stinchcombe, J.C., Majorovits, E., Bossi, G., Fuller, S. & Griffiths, G.M. Centrosome polarization delivers secretory granules to the immunological synapse. *Nature* **443**, 462-465 (2006).
- 935 10. de la Roche, M., Asano, Y. & Griffiths, G.M. Origins of the cytolytic synapse. *Nat Rev Immunol* **16**, 421-432 (2016).
11. de la Roche, M. *et al.* Hedgehog signaling controls T cell killing at the immunological synapse. *Science* **342**, 1247-1250 (2013).
- 940 12. Furmanski, A.L. *et al.* Tissue-derived hedgehog proteins modulate Th differentiation and disease. *J Immunol* **190**, 2641-2649 (2013).
- 945 13. Chan, V.S. *et al.* Sonic hedgehog promotes CD4<sup>+</sup> T lymphocyte proliferation and modulates the expression of a subset of CD28-targeted genes. *Int Immunol* **18**, 1627-1636 (2006).
14. Park, H.L. *et al.* Mouse Gli1 mutants are viable but have defects in SHH signaling in combination with a Gli2 mutation. *Development* **127**, 1593-1605 (2000).
- 950 15. Sekulic, A. *et al.* Efficacy and safety of vismodegib in advanced basal-cell carcinoma. *N Engl J Med* **366**, 2171-2179 (2012).
- 955 16. Esplugues, E. *et al.* Control of TH17 cells occurs in the small intestine. *Nature* **475**, 514-518 (2011).
17. Powrie, F., Leach, M.W., Mauze, S., Caddle, L.B. & Coffman, R.L. Phenotypically distinct subsets of CD4<sup>+</sup> T cells induce or protect from chronic intestinal inflammation in C. B-17 scid mice. *Int Immunol* **5**, 1461-1471 (1993).
- 960 18. Capone, A. & Volpe, E. Transcriptional Regulators of T Helper 17 Cell Differentiation in Health and Autoimmune Diseases. *Front Immunol* **11**, 348 (2020).
- 965 19. Miraldi, E.R. *et al.* Leveraging chromatin accessibility for transcriptional regulatory network inference in T Helper 17 Cells. *Genome Res* **29**, 449-463 (2019).
20. Katoh, Y. & Katoh, M. Hedgehog target genes: mechanisms of carcinogenesis induced by aberrant hedgehog signaling activation. *Curr Mol Med* **9**, 873-886 (2009).
- 970 21. Muranski, P. & Restifo, N.P. Essentials of Th17 cell commitment and plasticity. *Blood* **121**, 2402-2414 (2013).

22. Muranski, P. *et al.* Th17 cells are long lived and retain a stem cell-like molecular signature. *Immunity* **35**, 972-985 (2011).
- 975 23. Teperino, R. *et al.* Hedgehog partial agonism drives Warburg-like metabolism in muscle and brown fat. *Cell* **151**, 414-426 (2012).
24. Riobo, N.A., Saucy, B., Dilizio, C. & Manning, D.R. Activation of heterotrimeric G proteins by Smoothed. *Proc Natl Acad Sci U S A* **103**, 12607-12612 (2006).
- 980 25. Matissek, S.J. & Elswa, S.F. GLI3: a mediator of genetic diseases, development and cancer. *Cell Commun Signal* **18**, 54 (2020).
- 985 26. D'Amico, D. *et al.* Non-canonical Hedgehog/AMPK-Mediated Control of Polyamine Metabolism Supports Neuronal and Medulloblastoma Cell Growth. *Dev Cell* **35**, 21-35 (2015).
27. Blagih, J. *et al.* The energy sensor AMPK regulates T cell metabolic adaptation and effector responses in vivo. *Immunity* **42**, 41-54 (2015).
- 990 28. Nicholas, D.A. *et al.* Fatty Acid Metabolites Combine with Reduced beta Oxidation to Activate Th17 Inflammation in Human Type 2 Diabetes. *Cell Metab* **30**, 447-461 e445 (2019).
- 995 29. Javelaud, D. *et al.* TGF-beta/SMAD/GLI2 signaling axis in cancer progression and metastasis. *Cancer Res* **71**, 5606-5610 (2011).
30. Alvarez, J.I. *et al.* The Hedgehog pathway promotes blood-brain barrier integrity and CNS immune quiescence. *Science* **334**, 1727-1731 (2011).
- 1000 31. Harbour, S.N., Maynard, C.L., Zindl, C.L., Schoeb, T.R. & Weaver, C.T. Th17 cells give rise to Th1 cells that are required for the pathogenesis of colitis. *Proc Natl Acad Sci U S A* **112**, 7061-7066 (2015).
- 1005 32. Taipale, J. & Beachy, P.A. The Hedgehog and Wnt signalling pathways in cancer. *Nature* **411**, 349-354 (2001).
33. Liu, S. *et al.* Hedgehog signaling and Bmi-1 regulate self-renewal of normal and malignant human mammary stem cells. *Cancer Res* **66**, 6063-6071 (2006).
- 1010 34. Dierks, C. *et al.* Expansion of Bcr-Abl-positive leukemic stem cells is dependent on Hedgehog pathway activation. *Cancer Cell* **14**, 238-249 (2008).
- 1015 35. Clement, V., Sanchez, P., de Tribolet, N., Radovanovic, I. & Ruiz i Altaba, A. HEDGEHOG-GLI1 signaling regulates human glioma growth, cancer stem cell self-renewal, and tumorigenicity. *Curr Biol* **17**, 165-172 (2007).

- 1020 36. Peacock, C.D. *et al.* Hedgehog signaling maintains a tumor stem cell compartment in multiple myeloma. *Proc Natl Acad Sci U S A* **104**, 4048-4053 (2007).
37. Bartlett, H.S. & Million, R.P. Targeting the IL-17-T(H)17 pathway. *Nat Rev Drug Discov* **14**, 11-12 (2015).
- 1025 38. Pacha, O., Sallman, M.A. & Evans, S.E. COVID-19: a case for inhibiting IL-17? *Nat Rev Immunol* **20**, 345-346 (2020).
39. De Biasi, S. *et al.* Marked T cell activation, senescence, exhaustion and skewing towards TH17 in patients with COVID-19 pneumonia. *Nat Commun* **11**, 3434 (2020).
- 1030 40. Huh, J.R. *et al.* Digoxin and its derivatives suppress TH17 cell differentiation by antagonizing ROR $\gamma$  activity. *Nature* **472**, 486-490 (2011).
41. Mele, D.A. *et al.* BET bromodomain inhibition suppresses TH17-mediated pathology. *J Exp Med* **210**, 2181-2190 (2013).
- 1035 42. Cheung, K. *et al.* BET N-terminal bromodomain inhibition selectively blocks Th17 cell differentiation and ameliorates colitis in mice. *Proc Natl Acad Sci U S A* **114**, 2952-2957 (2017).
- 1040 43. Brownell, I., Guevara, E., Bai, C.B., Loomis, C.A. & Joyner, A.L. Nerve-derived sonic hedgehog defines a niche for hair follicle stem cells capable of becoming epidermal stem cells. *Cell Stem Cell* **8**, 552-565 (2011).
- 1045 44. Skjoedt, M.O. *et al.* Two mannose-binding lectin homologues and an MBL-associated serine protease are expressed in the gut epithelia of the urochordate species *Ciona intestinalis*. *Dev Comp Immunol* **34**, 59-68 (2010).
45. Dobin, A. *et al.* STAR: ultrafast universal RNA-seq aligner. *Bioinformatics* **29**, 15-21 (2013).
- 1050 46. Liao, Y., Smyth, G.K. & Shi, W. The Subread aligner: fast, accurate and scalable read mapping by seed-and-vote. *Nucleic Acids Res* **41**, e108 (2013).
- 1055 47. Love, M.I., Huber, W. & Anders, S. Moderated estimation of fold change and dispersion for RNA-seq data with DESeq2. *Genome Biol* **15**, 550 (2014).
48. Subramanian, A. *et al.* Gene set enrichment analysis: a knowledge-based approach for interpreting genome-wide expression profiles. *Proc Natl Acad Sci U S A* **102**, 15545-15550 (2005).
- 1060 49. Adolph, T.E. *et al.* Paneth cells as a site of origin for intestinal inflammation. *Nature* **503**, 272-276 (2013).



# Figures

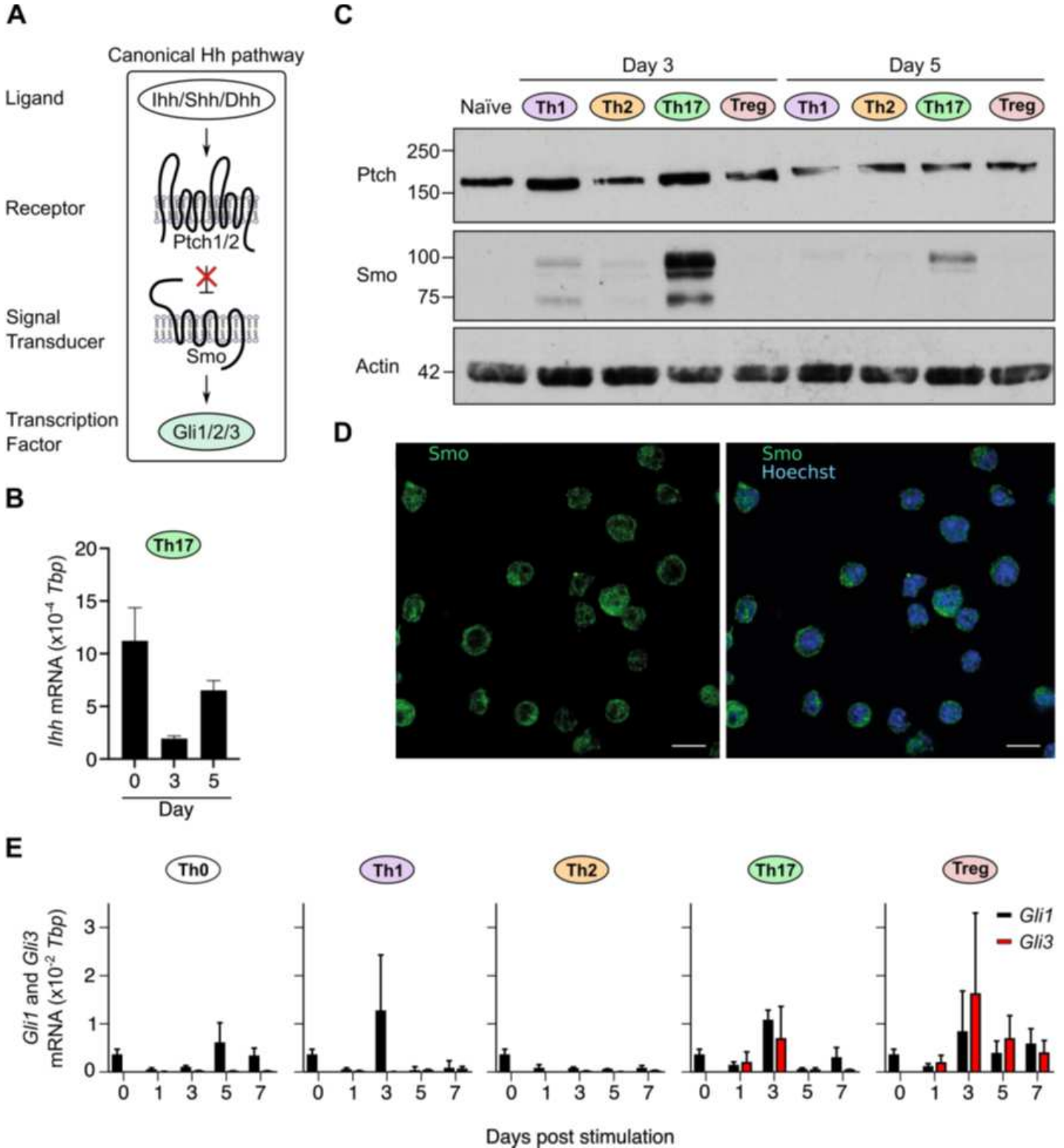


**Figure 1**

Key Hedgehog signaling components are induced in Th17 cells. (A) Overview of canonical Hh signaling. (B-E) Naïve CD4<sup>+</sup> T cells were purified from spleen and peripheral lymph nodes of C57BL/6 mice and stimulated with plate-bound anti-CD3e/CD28 antibodies in the presence of polarizing cytokines to

generate Th0, Th1, Th2, Th17 and Treg subsets. (B) Expression of *Ihh* was assessed by qRT-PCR in naïve CD4<sup>+</sup> T cells and Th17 cells at the indicated timepoints after TCR stimulation. Data is normalized to *Tbp* as a reference gene. n = 3 independent experiments. (C) Immunoblot analysis of *Ptch* and *Smo* in naïve CD4<sup>+</sup> T cells and T helper (Th) subsets at indicated timepoints post stimulation. n = 2 (naïve) or 3 (Th subsets) independent experiments. (D) Immuno-fluorescence imaging (single x-y confocal section) of Th17 cells at day 3 labelled with antibodies against *Smo* (green). Nuclei were stained with Hoechst (blue). Scale bars: 10µm. (E) Expression of *Gli1*, *Gli2* and *Gli3* were assessed by qRT-PCR in Th subsets at indicated timepoints post stimulation in the presence of polarizing cytokines. Data is normalized to *Tbp* as a reference gene with similar results obtained when using *CD3e* as a reference gene. n = 3 independent experiments. *Gli2* mRNA was undetectable in all conditions tested.

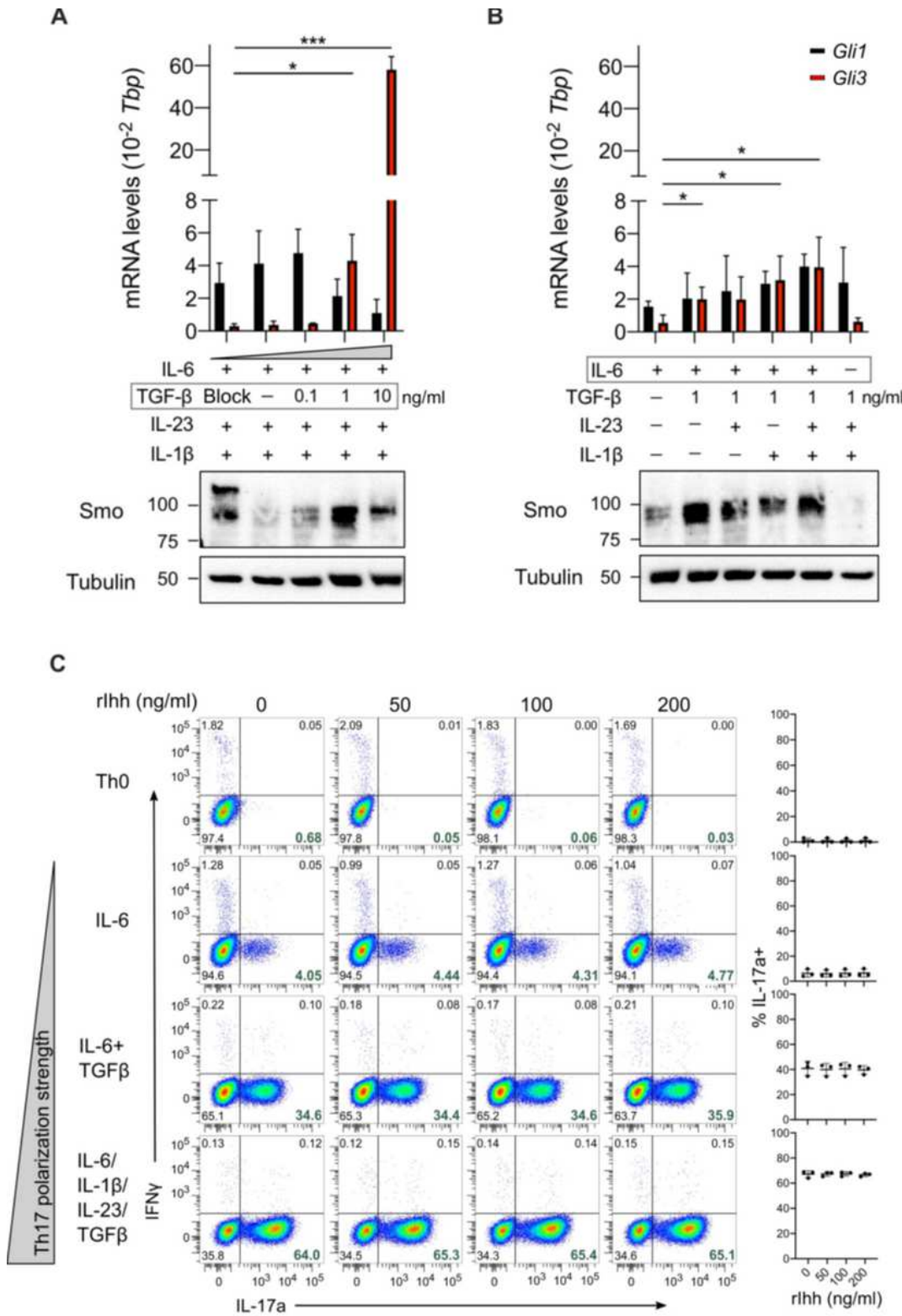


**Figure 2**

IL-6 and TGF $\beta$  but not exogenous lhh ligand are the primary inducers of Hh signaling in Th17 cells. (A-C) Naïve CD4 $^{+}$  T cells were purified from spleen and peripheral lymph nodes of C57BL/6 mice and polarized with the indicated polarizing cytokines. (A, B) Cells were harvested at day 3 post stimulation for immunoblot analysis of Smo and qRT-PCR analysis of Gli1 and Gli3. TGF $\beta$  blocking antibody (clone: 1D11) was added in the indicated condition for the duration of polarization at 10 $\mu$ g/ml. Data is

normalized to Tbp as a reference gene. Similar results were obtained when CD3e was used as a reference gene. n = 3 independent experiments. (C) Naive CD4<sup>+</sup> T cells were stimulated with the indicated polarizing cytokines in the presence or absence of recombinant N-terminal murine Ihh fragment at the indicated concentrations. All cells were polarized in the presence of anti-IFN $\gamma$  and anti-IL4 blocking antibodies and were harvested for analysis by FACS on day 5. Representative flow cytometry plots of n = 3 independent experiments are shown with a summary on the right. Data are means  $\pm$  SD. p-values were calculated using an unpaired two-tailed Student's t test. \* p<0.05, \*\* p<0.01, \*\*\* p<0.001.

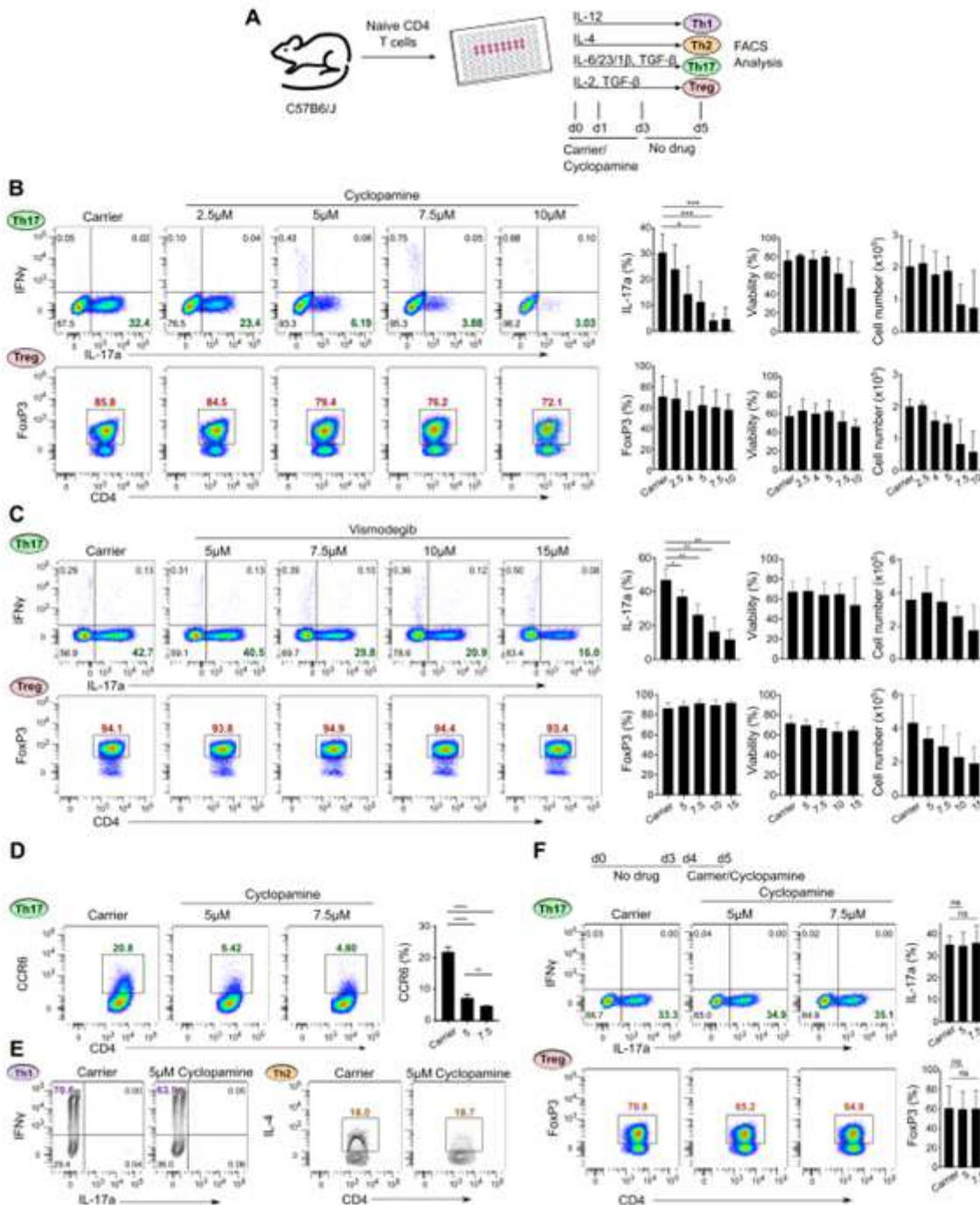
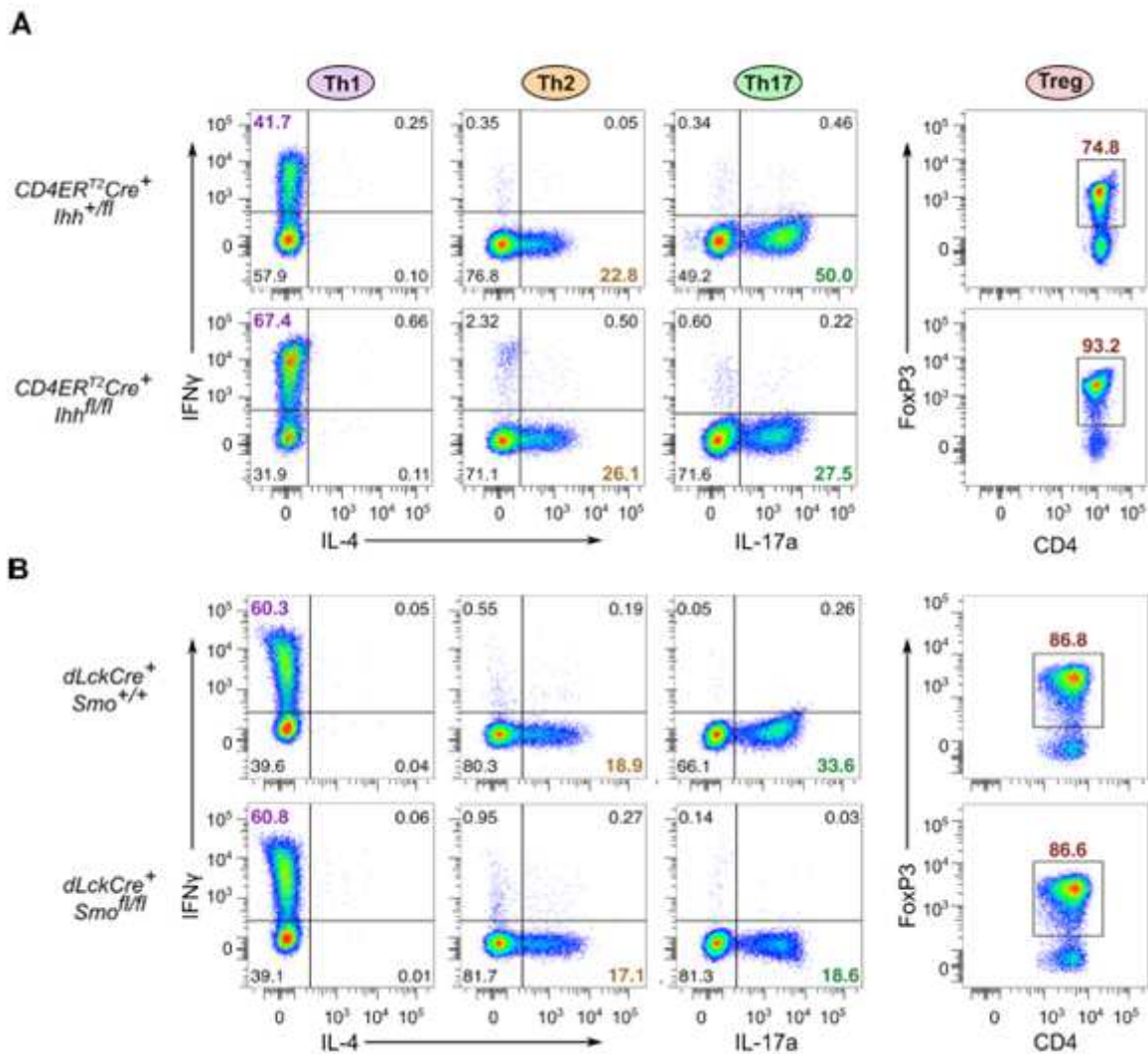


Figure 3

Small molecule Hh inhibitors selectively block Th17 polarization in vitro. (A) Schematic overview of Hh inhibitor cyclopamine administration schedule. (B) Naïve CD4<sup>+</sup> T cells were stimulated under Th17 or Treg polarizing conditions in the presence of the indicated doses of cyclopamine or carrier control for three days. Cells were harvested for analysis by flow cytometry on day 5. Quantitation of IL-17a/FoxP3 expression, viability measured by absence of live/dead staining, and cell numbers are shown on the right. n = 4 independent experiments. (C) Naïve CD4<sup>+</sup> T cells were stimulated under Th17 or Treg polarizing conditions in the presence of the indicated doses of vismodegib or carrier control for five days. Cells were harvested for analysis by flow cytometry on day 5. Quantitation of IL-17a/FoxP3 expression, viability measured by absence of live/dead staining, and cell numbers are shown on the right. n = 3 independent experiments. (D) Naïve CD4<sup>+</sup> T cells were stimulated under Th17 polarizing conditions in the presence of the indicated doses of cyclopamine or carrier control for three days. Cells were harvested for analysis by flow cytometry on day 5. Quantitation of cell-surface CCR6 is shown on the right. n = 3 independent experiments. (E) Naïve CD4<sup>+</sup> T cells were stimulated under Th1 or Th2 polarizing conditions in the presence of 5µM cyclopamine or carrier control for three days. Cells were harvested for analysis by flow cytometry on day 5. n = 3 independent experiments. (F) Naïve CD4<sup>+</sup> T cells were stimulated under Th17 or Treg polarizing conditions in the presence of the indicated dose of cyclopamine or carrier control for the final 24h of polarization. Cells were harvested for analysis by flow cytometry on day 5. n = 3 independent experiments. Data are means +/- SD. p-values were calculated using an unpaired two-tailed Student's t test. \* p<0.05, \*\* p<0.01, \*\*\* p<0.001.



**Figure 4**

Conditional knockout of Hh signaling components *Ihh* and *Smo* in CD4<sup>+</sup> T cells leads to diminished Th17 polarization but does not affect other Th lineages. Naïve CD4<sup>+</sup> T cells were purified from spleen and peripheral lymph nodes of either CD4ERT2Cre<sup>+</sup> *Ihh*<sup>+/fl</sup> (HET) and *Ihh*<sup>fl/fl</sup> (KO) C57BL/6 mice (A), or dLckCre<sup>+</sup> *Smo*<sup>+/+</sup> (WT) and dLckCre<sup>+</sup> *Smofl/fl* (KO) C57BL/6 mice (B). (A,B) Cells were stimulated under Th1, Th2, Th17 or Treg polarizing conditions and harvested for analysis by flow cytometry on day 5. n=2-3 mice per genotype.

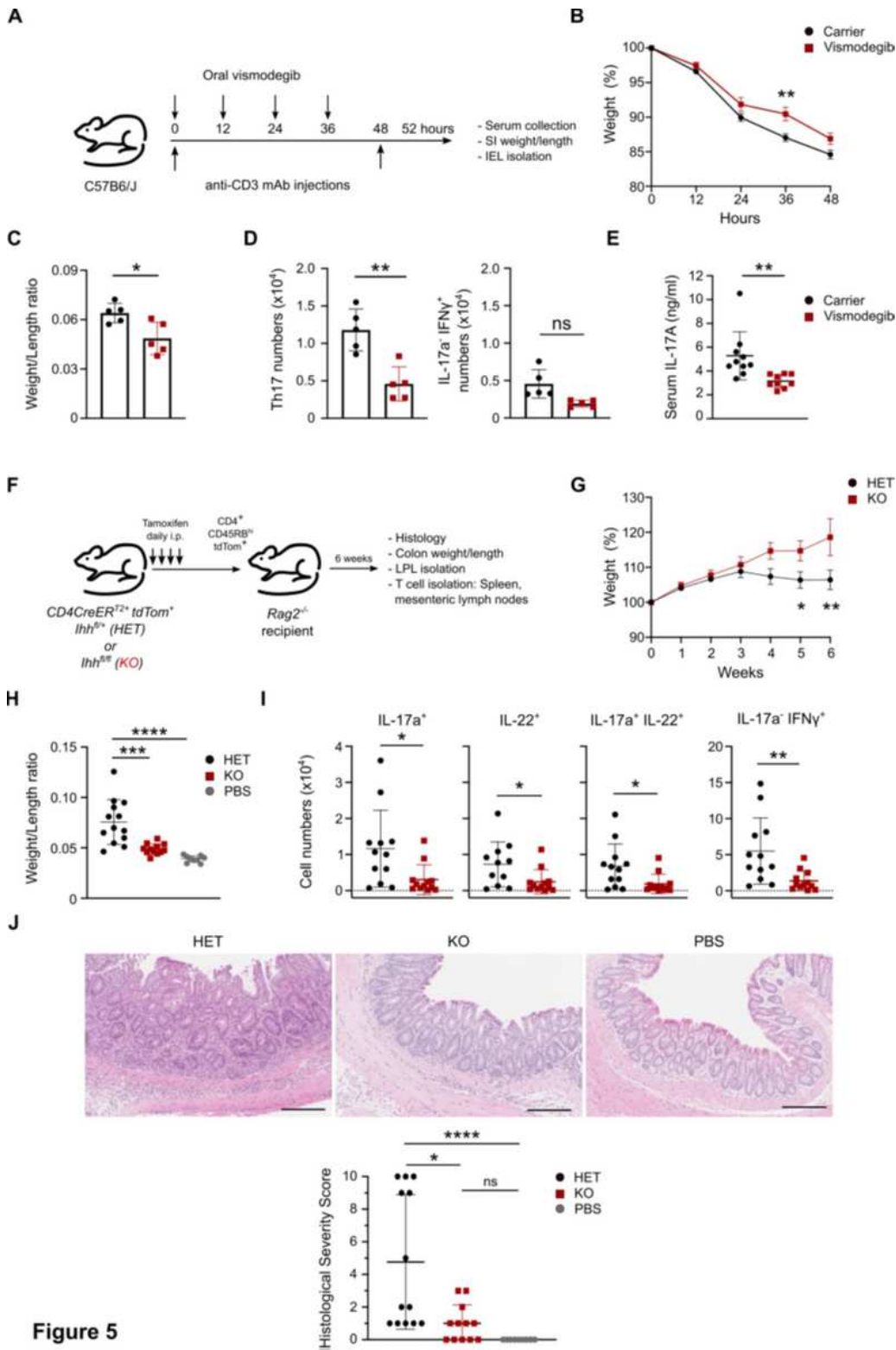


**Figure 5**

**Figure 5**

Hh signaling is critical for Th17 responses in vivo. (A) C57BL/6 mice were injected i.p. with 20  $\mu$ g anti-CD3 monoclonal antibody (Clone: 145-2C11) at 0h and 48h and dosed every 12h by oral gavage with 100 mg/kg vismodegib or carrier control. Mice were harvested at 52h. (B) Weight loss during the course of the experiment. Pooled data from three independent experiments. (C) Small Intestine weight/length ratios. Representative data shown from one of three independent experiments. (D) IEL Th17 and IFN $\gamma$ + IL-17a-

CD4<sup>+</sup> T cell numbers. Representative data shown from one of three independent experiments. Gating strategy is shown in Suppl. Fig. 7. (E) Serum IL-17a concentrations at 52h. Pooled data from three independent experiments. p-values were calculated using an unpaired two-tailed Student's t test. \* p<0.05, \*\* p<0.01. (F) Rag2<sup>-/-</sup> mice were injected i.p. with 4x10<sup>5</sup> CD45RB<sup>hi</sup> CD25<sup>neg</sup> tdTom<sup>+</sup> CD4<sup>+</sup> T cells isolated from the spleens and peripheral lymph nodes of CD4ERT2Cre Ihhfl<sup>+/+</sup> (HET) or CD4ERT2Cre Ihhfl<sup>fl/fl</sup> (KO) mice. Mice were harvested at 6-7 weeks. (G-J) pooled data from three independent experiments shown. (G) Weight loss during the course of the experiment. (H) Colon weight/length ratios. (I) Numbers of IL-17a<sup>+</sup>, IL-22<sup>+</sup>, IL-17a<sup>+</sup> IL-22<sup>+</sup>, IFN $\gamma$ <sup>+</sup> IL-17a<sup>neg</sup> T cells isolated from colonic lamina propria. Gating strategy is shown in Suppl. Fig. 8. (J) Panels on the top show representative H&E staining of the recipient mouse colons. Panel on the bottom shows quantification of histological severity scored blindly by a gastroenterologist. Scale bars: 200 $\mu$ m. Data are means +/- SEM (B,G). Rest are means +/- SD. p-values were calculated using an unpaired two-tailed Student's t test. \* p<0.05, \*\* p<0.01, \*\*\* p<0.001. (J) p-values were calculated using an unpaired two-tailed Student's t test (C,D,E,I), a Kruskal-Wallis test (J), a one-way ANOVA (H) or a two-way ANOVA with Sidak correction (B,G). \* p<0.05, \*\* p<0.01, \*\*\* p<0.001.

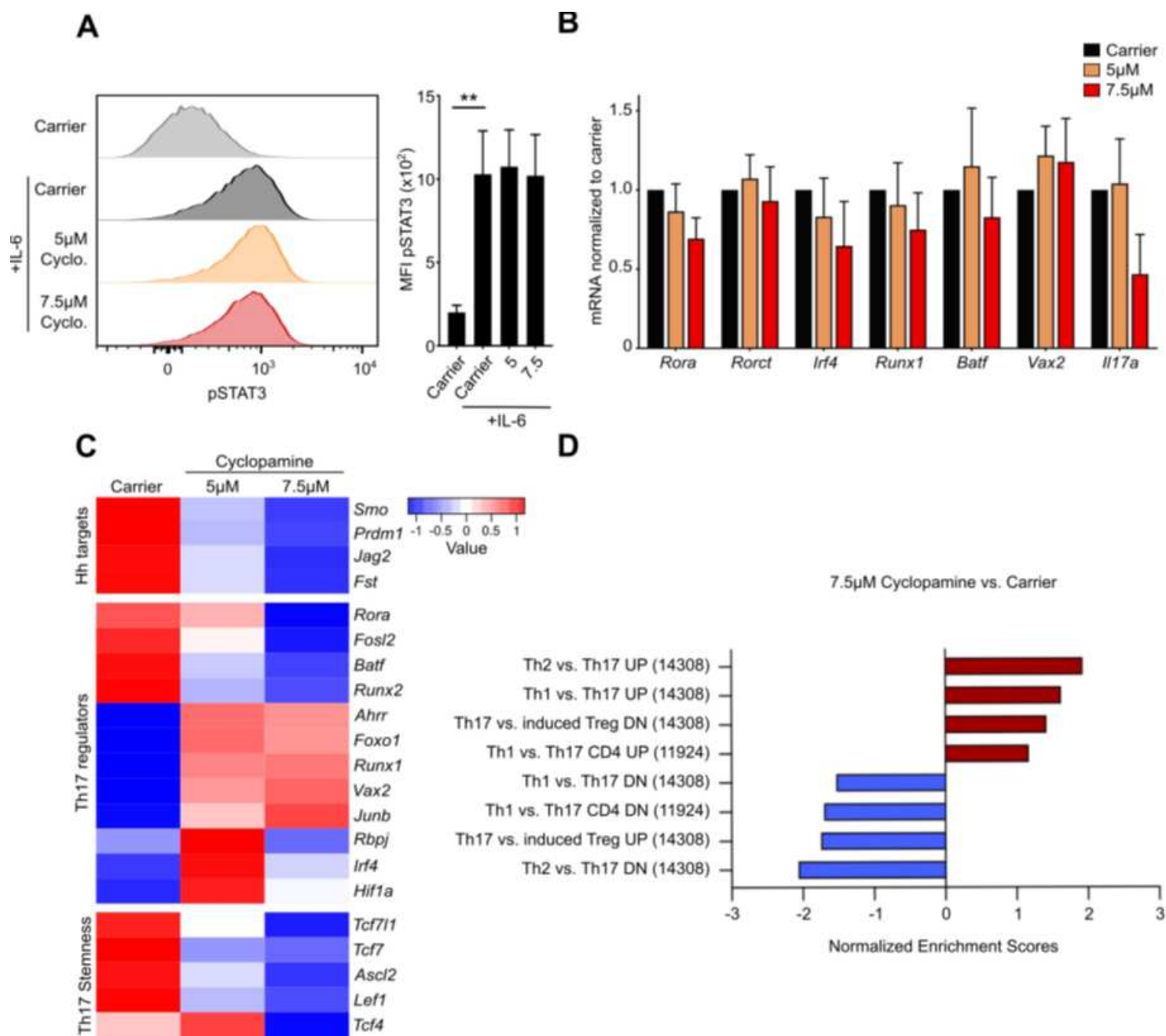


**Figure 6**

Mechanistic analysis of Th17-related signaling nodes. Naïve CD4<sup>+</sup> T cells were purified from spleen and peripheral lymph nodes of C57BL/6 mice and stimulated under Th17 polarizing conditions in the presence of the indicated doses of cyclopamine or carrier control for three days. (A) On day 5, cells were treated with 100ng/ml IL-6 for 15min and harvested for analysis of pSTAT3 levels by flow cytometry. Quantitation of pSTAT3 staining is shown on the right. n = 3 independent experiments. (B) Cells were harvested for analysis at day 3. Expression of RORa, RORct, IRF4, Runx1, BATF, Vax2 and Il17a were analyzed by qRT-PCR. Data is normalized to Tbp as a reference gene. Similar results were obtained when CD3e was used as a reference gene. n = 3 independent experiments. (C) RNASeq analysis of Hh target genes, Th17 regulators and stemness genes. Th17 cells were polarized as described above stimulated in the presence of the indicated doses of cyclopamine or carrier control for three days and harvested at day

3. Six samples/group. (D) Normalized Enrichment Scores (NES) from GSEA of (C) demonstrating a loss of Th17 identity upon Hh inhibitor treatment. Data are means  $\pm$  SD. p-values were calculated using an unpaired two-tailed Student's t test. \*\* indicates  $p < 0.01$ .

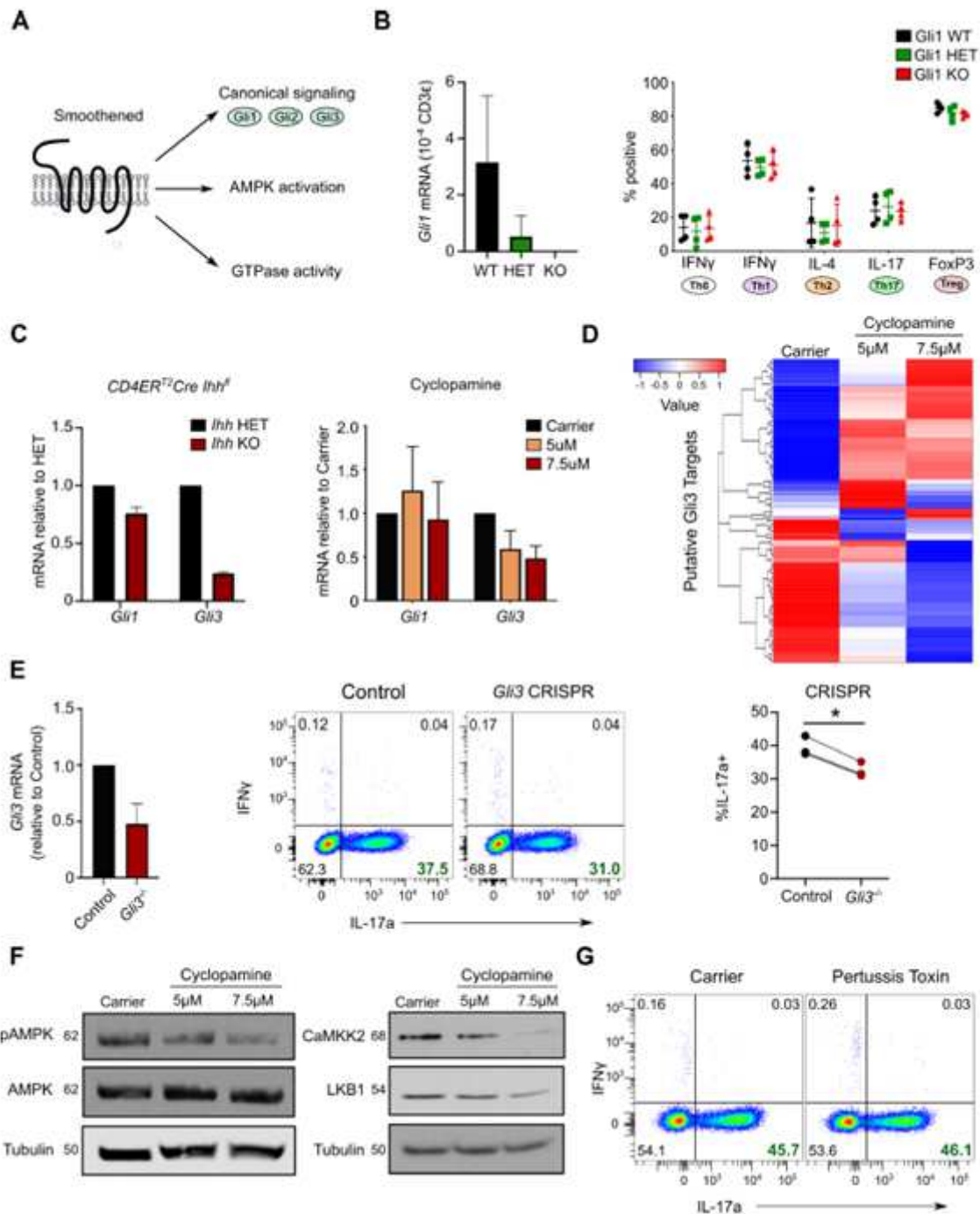


**Figure 7**

Canonical and non-canonical Hh signaling contribute to Th17 polarization. (A) Schematic overview of canonical and non-canonical Hedgehog signaling. (B) Naïve CD4<sup>+</sup> T cells were purified from spleen and peripheral lymph nodes of Gli1eGFP<sup>+/+</sup> (WT), Gli1eGFP<sup>+/-</sup> (HET) or Gli1eGFP<sup>-/-</sup> (KO) mice. Cells were stimulated under Th0, Th1, Th2, Th17 or Treg polarizing conditions. Cells were assessed for expression of Gli1 RNA on day 3 (Th17, left) or harvested for analysis by flow cytometry on day 5 (right). n = 4 mice per

genotype. No statistically significant differences in cytokine production were observed between genotypes. (C) Analysis of Gli1 and Gli3 expression by qRT-PCR of Th17 cells on day 3. Panel on the left shows Th17 cells polarized from CD4ERT2Cre+ Ihh+/fl (HET) or CD4ERT2Cre+ Ihhfl/fl (KO) mice. Panel on the right shows Th17 cells polarized from C57BL/6 mice in the presence of the indicated dose of cyclopamine or carrier control for three days. Data are normalized to Tbp as a reference gene. Similar results were obtained when CD3e was used as a reference. n = 2-3 independent experiments. (D) Expression of all putative Gli3 target genes as predicted by Miraldi et al. (2019) in RNA-Seq analysis from Fig. 6C. Th17 cells were polarized as described above stimulated in the presence of the indicated doses of cyclopamine or carrier control for three days and harvested at day 3. Six samples/group (E-G) Naïve CD4+ T cells were purified from spleen and peripheral lymph nodes of C57BL/6 mice and stimulated under Th17 polarizing conditions. (E) After 24h CRISPR/Cas9 RNP complexes targeting Gli3 were electroporated. Cells were harvested for qRT-PCR analysis of Gli3 at day 3 (left panel) and for analysis by flow cytometry on day 5 (middle panel). Quantitation of IL-17a expression is shown on the right. n = 3 independent experiments. (F) Naïve CD4+ T cells were stimulated in the presence of the indicated doses of cyclopamine or carrier control for three days. Immunoblot analysis of Th17 cells on day 3 for pAMPK, AMPK, CaMKK2, LKB1 and Tubulin is shown. n = 3 independent experiments. (G) Naïve CD4+ T cells were stimulated in the presence of 100ng/ml pertussis toxin or carrier control for five days. Cells were analyzed by flow cytometry on day 5. n = 3 independent experiments. Data are means +/- SD. p-values were calculated using an unpaired two-tailed Student's t test. \* p<0.05, \*\* p<0.01, \*\*\* p<0.001.

## Supplementary Files

This is a list of supplementary files associated with this preprint. Click to download.

- [NCBSupplementCOMPRESS.pdf](#)